APPROVED FOR RELEASE: 2007/02/08: CIA-RDP82-00850R000200030011-4

JPRS L/8801

5 December 1979

USSR Report

PHYSICS AND MATHEMATICS

(FOUO 6/79)

Quantum Electronics

FBIS FOREIGN BROADCAST INFORMATION SERVICE

FOR OFFICIAL USE ONLY

APPROVED FOR RELEASE: 2007/02/08: CIA-RDP82-00850R000200030011-4

NOTE

JPRS publications contain information primarily from foreign newspapers, periodicals and books, but also from news agency transmissions and broadcasts. Materials from foreign-language sources are translated; those from English-language sources are transcribed or reprinted, with the original phrasing and other characteristics retained.

Headlines, editorial reports, and material enclosed in brackets [] are supplied by JPRS. Processing indicators such as [Text] or [Excerpt] in the first line of each item, or following the last line of a brief, indicate how the original information was processed. Where no processing indicator is given, the information was summarized or extracted.

Unfamiliar names rendered phonetically or transliterated are enclosed in parentheses. Words or names preceded by a question mark and enclosed in parentheses were not clear in the original but have been supplied as appropriate in context. Other unattributed parenthetical notes within the body of an item originate with the source. Times within items are as given by source.

The contents of this publication in no way represent the policies, views or attitudes of the U.S. Government.

For further information on report content call (703) 351-2938 (economic); 3468 (political, sociological, military); 2726 (life sciences); 2725 (physical sciences).

APPROVED FOR RELEASE: 2007/02/08: CIA-RDP82-00850R000200030011-4

JPRS L/8801

5 December 1979

USSR REPORT

PHYSICS AND MATHEMATICS

(FOUO 6/79)

QUANTUM ELECTRONICS

Moscow KVANTOVAYA ELEKTRONIKA in Russian Vol 6, No 8, Aug 79
pp 1626-1638, 1690-1697, 1705-1711, 1773-1777, 1816-1818

CONTENTS

LASERS AND MASERS

UDC 621.373.826.038.823

THEORY OF AN ELECTRON PHOTOTRANSITION CHEMICAL LASER WITH THERMAL INITIATION BEHIND THE SHOCK WAVE FRONT

Moscow KVANTOVAYA ELEKTRONIKA in Russian Vol 6 No 8, Aug 79 pp 1626-1638
manuscript received 19 Oct 78

[Article by I.A. Izmaylov, V.A. Kochelap, Yu.A. Kukibnyy and S.I. Pekar, Ukrainian SSR Academy of Sciences Institute of Semiconductors, Kiev]

[Text] The theory is developed for a steady-state electron phototransition chemical laser initiated by a shock wave in a dense flow of reagents. A calculation is made of the inverse population density behind the front of the shock wave for the case of photorecombination reactions. Proof is given of the origin of a waveguide localizing the working mode of the laser in the inversion zone. The light gain, α, in waveguide modes is calculated. For laser generation conditions in gas dynamics and chemical kinetics the light-stimulated chemical reaction is taken into account, which alters the spatial relationships of the density, temperature, flow rate and concentrations of reagents. A determination is made of the unit light power, P, drawn off from the flow as a function of light losses. A number of specific gas mixtures are discussed and three of the most promising have been selected for use in lasers: NO_2Cl-Ar, O_3-Ar and O_3-CO. It is demonstrated that for these inversion originates over a broad wavelength range and the conditions for the origin of a waveguide are compatible with the conditions for the formation of inversion. For these mixtures have been obtained $\alpha \gtrsim 10^{-3}$ cm^{-1} and a power of approximately 100 kW per square centimeter of the gas flow.

1. Introduction

The upper limit of the power of a chemical laser in the steady-state mode is determined by the density of the flux of chemical energy supplied to it. With this energy, separated in the elementary event of the reaction, the power supplied is proportional to the density of the gas mixture and its rate of flow. With a supersonic flow rate of 3 km/s, a normal gas density and energy released in the elementary event of 2 eV, the flux density of the chemical energy equals approximately 3 MW/cm^2. In order for a laser to possess high efficiency, it is sufficient that the energy of an emitted photon be comparable to the energy released in the elementary event of the reaction, which is possible with electron phototransitions, and that the quantum yield of the

stimulated emission be on the order of one.* The latter condition can be fulfilled in lasers where the parallel reaction channels are a thermal and radiation channel (cf., e.g., [1,2]). By stimulating the reaction's radiation channel, its dominance over the thermal can be achieved even in the case when the quantum yield of spontaneous emission is low. Then the velocity of the laser process will be determined by the rate of exhaustion of reagents (for a photorecombination laser, by the rate of exhaustion of atoms and radicals). The theory of chemical lasers utilizing electron phototransitions at high pressures was considered in [3-8], but such lasers have still not been implemented experimentally.

In another group of studies devoted to the creation of chemical electron phototransition lasers studies were made of exchange reactions between metals and oxidants [9]. The quantum yield in these reactions is high (0.15 to 0.6) even in spontaneous chemiluminescence. However, with an increase in pressure beginning with a few mm Hg the quantum yield drops substantially. And in this group of studies it has still not been possible to achieve inversion [10].

In this paper the theory is developed for steady-state lasers operating with an initial gas mixture pressure on the order of 1 atm and higher, when the time for the occurrence of the thermal chemical reaction is not longer than 1 μs and the length of the reaction zone along the flow is less than 1 mm. It is necessary that the reaction not be able to take place during the relatively long period of mixing and supplying the mixture to the cavity. For this purpose the temperature of the mixture in the supplying gas line must be so low that a reaction does not occur at this temperature. The reaction must be stimulated within the optical cavity itself during periods much shorter than 1 ms. This can be accomplished by a sudden increase in the temperature of the gas (of thousands of degrees in 0.1 ns) in the front of the shock wave (UV) created inside the cavity [11].

Usually the length of the inversion and laser generation zone is shorter than the thermal reaction zone. In particular, in a laser of the type in [1,2] the stimulated radiation reaction must outdistance the thermal and as a result of this the length of its zone can equal a few dozen wavelengths of the light. With these thicknesses of the active layer diffraction losses of photons and losses associated with distortion of the active layer become substantial. As a result of these losses generation generally could prove to be impossible [5,6]. However, behind the front of the shock wave in the reaction zone arises a layer of increased densities and refractive indices of the gas, which can act as a plane waveguide localizing the laser's operating mode in the inversion zone and eliminating these losses of photons [12].

Below are discussed only reactions of radiative recombination of atoms and radicals. The latter react rapidly even at low temperatures; therefore they

*Another possibility for achieving high efficiency of the laser process involves the utilization of photons of not too high energy with a quantum yield of stimulated emission per single reaction event of greater than one. For example, a cascade of stimulated vibrational-rotational phototransitions.

cannot be present in the supplying flow. These radicals must be rapidly and in great quantity created inside the optical cavity, e.g., by the thermal dissociation of stable molecules behind the front of the shock wave.

In this paper the theory of the shock wave is developed and of the unidimensional steady-state gas dynamical flow, taking into account the kinetics of chemical reactions in the gas. It differs from the familiar theory in [13] by taking account in kinetics of the light-stimulated radiation reaction, which alters the spatial relationships of density, temperature, flow rate and concentrations of components of the gas mixture. Then are calculated the spatial behavior of the complex dielectric constant and the lowest modes of the plane waveguide originating behind the shock wave front. A determination is made of the gain (absorption) of light in these modes as a function of the pressure, velocity and composition of the initial gas stream. The output light power is obtained, derived from a unit area of the cross section of the incoming flow. The theory developed is applied to 12 specific gas mixtures from which have been selected three of the most promising: NO_2Cl-Ar, O_3-Ar and O_3-CO.

2. Investigation of the Gas Dynamics, Chemical Kinetics and Properties of the Waveguide, Taking Into Account the Laser Process

Of the 12 mixtures considered in this paper seven react according to the following scheme. A gas consisting of molecules AX is thinned by inert gas M; after a sudden rise in temperature the following reactions take place:

$$AX + M = A + X + M - Q_1, \tag{1}$$

$$AX + X = A + X_2, \tag{2}$$

$$X + X + M = X_2 + M + \begin{cases} \hbar\omega \\ Q_3 \end{cases}, \tag{3}$$

where Q equals the heat of the reactions. It is assumed that at the temperature considered particles of A do not dissociate and do not form compounds of A_2. Reaction (3) takes place through competing radiation and thermal channels.

Designating the partial concentration of gases as [AX], [X], [A], [X_2] and [M], the density of the mixture by ρ, the temperature by T and the velocity by v, we write the laws for the conservation of mass, momentum and energy in the absence of laser generation:

$$\rho v = \rho_0 v_0, \tag{4}$$

$$p + \rho v^2 = p_0 + \rho_0 v_0^2, \tag{5}$$

$$^1/_2 v^2 + h = ^1/_2 v_0^2 + h_0, \tag{6}$$

where p is the pressure of the gas mixture; subscript 0 indicates the initial state of the gas flowing into the shock wave front; and $h = c_p T + (1/\rho)\{Q_1[X] + (2Q_1 - Q_3)[X_2]\}$ is the enthalpy (c_p is the specific heat, depending on concentration). The specific heat of each component of the mixture is considered constant. We disregard spontaneous emission in (3). Equations for the balance of matter have the form

$$[AX] + [X] + 2[X_2] = [AX] + [A] = (\rho/\rho_0)[AX]_0. \tag{7}$$

As a result it is sufficient to write kinetic equations for just two concentrations:

$$\frac{d}{dx}([X]v) = W_1 - W_2 - W_3, \tag{8}$$

$$\frac{d}{dx}([X_2]v) = W_2 + \frac{1}{2}W_3, \tag{9}$$

where

$$\begin{aligned} W_1 &= k_1[M]([AX] - [A][X]/K_1); \\ W_2 &= k_2([AX][X] - [A][X_2]K_3/K_1); \\ W_3 &= k_3([X]^2 - K_3[X_2])[M]; \end{aligned} \tag{10}$$

$k_{1,2,3}$ represents reaction rate constants; and K_1 and K_3, equilibrium constants of reactions (1) and (3). It is assumed that although the concentrations of components are considerably unbalanced, thermal equilibrium exists in all degrees of freedom of the motion of molecules. Coordinate x points along the flow. Plane $x = 0$ represents the front of the shock wave. In the region of $x < 0$, $[AX]_0$ and $\eta = [AX]_0/[M]_0$ are assigned and $[X] = [A] = [X_2] = 0$.

Solution of Gas Dynamics and Kinetics Equations in the Absence of Laser Generation

For the purpose of investigating the possibility of achieving high concentrations of atoms and radicals, as well as an inverse population density in the laser's initiation of a shock wave, equations (4) to (10) have been solved numerically for many values of the parameters included in them. Employed have been values of $k_1 = 10^{-9} \exp[-Q_1/(RT)]$ cm^3/s, $k_2 = 10^{-11}$ cm^3/s,

$k_3 = 10^{-33}$ cm^6/s $_3K_1 = 10^{25} \exp [-Q_1/(RT)]$ cm^{-3} , and $K_3 = 10^{24} \exp$ $\exp [-Q_3/(RT)]$ cm^{-3} , which is typical of fast reactions at high temperatures [14]. As a result, e.g., with $Q_1 = 35$ kcal/mole , $Q_3 = 100$ kcal/mole , $p_0 = 5$ atm , and $T_0 = 300°K$, and

$$\text{with a Mach number of } M = 5.5 \text{ , } \eta = 0.1 \text{ ,} \tag{11}$$

the dependences have been obtained which are shown in fig 1, where curves 1 to 3 represent the spatial behavior of relative concentrations of components determined from the equation $C_B = [B]/([M]\eta)$. Curve 1 shows that dissociation and the disappearance of original molecules of AX take place in a zone whose length is on the order of 1 μ. Curve 3 shows that in the same zone are formed atoms of X needed for working laser reaction (3); their concentration, C_X , reaches a maximum value of 0.45, whereas its equilibrium value with $x \to \infty$ equals 0.014. C_X is fairly high in a zone 10 to 20 μ long. Curve 2 shows the monotonic growth in the concentration of products X_2.

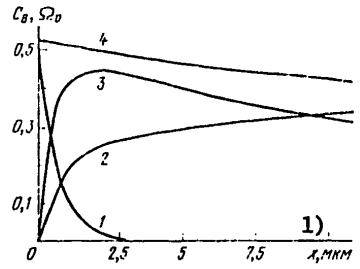

Figure 1. Dependences of Flow Characteristics on Distance to the Shock Wave Front: 1--1/2 C_{AX}; 2--C_{X_2}; 3--C_X; 4--Ω_v

Key:
1. X, μ

In lasers of the type considered (if, e.g., radiative combination takes place from a continuous spectrum) it is feasible to term inverse the case when for a specific frequency of ω per unit of time the number of radiation events is greater than the number of absorption events. The test for this inversion has the form [3]:

$$[X]^2 \geqslant [X_2] K_3(T) \exp(\hbar\omega/kT). \tag{12}$$

It is obvious from this equation that with assigned concentrations and temperature there exists a violet frequency limit (maximum frequency), ω_v , below which inversion exists. With $\omega = \omega_v$ (12) is converted into an equality.

In fig 1 curve 4 represents the spatial behavior of the magnitude $\Omega_v = \hbar\omega_v/Q_3$. From it it is obvious that inversion is possible with $\hbar\omega \gtrsim 2$ eV .

Fig 1 illustrates the favorable possibility for accomplishment of the process under conditions when the inversion zone is much longer than the zone for initiation of the working reaction. For efficiency of the laser it is also important that inversion exist in a zone on the order of 10 μ and that the concentration of reaction products X_2 be still not too high. As a maximum $[X] \gtrsim 2 \cdot 10^{19}$ cm^{-3} .

Curves similar to those presented in fig 1 were calculated for different combinations of parameters Q_1 , η , p_0 and M . Since it is impossible to present the entire diversity of individual graphs, let us show only the maximum ordinates of curves for C_X and Ω_v (fig 2). It is obvious from fig 2 that if with fixed M p_0 is increased, then C_X almost does not change (is slightly reduced). With an increase in M , C_X increases substantially, as also with a reduction in Q_1 and η .

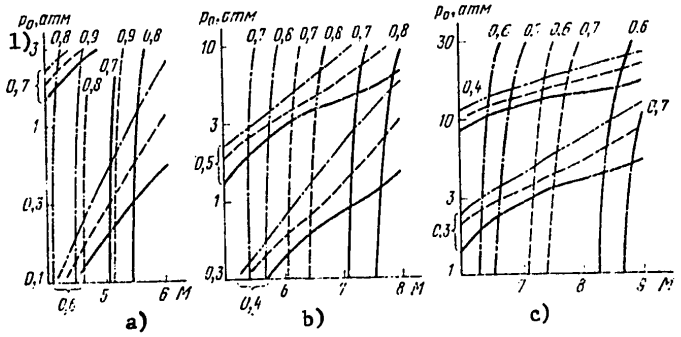

Figure 2. Maximum Values of C_X and Ω_v for Q_1 = 20 (a), 35 (b) and 50 kcal/mole (c); η = 0.2 (solid line), 0.1 (dotted line) and 0.5 (dash-dot line); Q_3 = 100 kcal/mole; as well as for different values of p_0 and M . The nearly vertical lines correspond to constant values of C_X^{max} , indicated above the curves, and the sloping lines to constant values of Ω_v^{max} , indicated on the curves.

Key:
1. p_0 , atm

The violet inversion boundary, Ω_v , increases with an increase in p_0 and η and with a reduction in Q_1 and M . In order, with assigned Q_1 and η , for C_X to be greater than a given value, it must lie in plane p_0, M to the right of the corresponding nearly vertical curve. In order for Ω_v to exceed a given value it must lie above the corresponding sloping curve. A comparison of fig 2a to 2c shows that for the purpose of achieving favorable values of C_X and Ω_v it is necessary to select low Q_1 . With $Q_1/Q_3 >$ > 0.5 process (1) to (3) becomes endothermic.

According to the Chapman-Jouguet equation [13], for each value of heat release in the exothermic process there exists a lower limit of M with which the flow of gas from the shock wave can still be steady-state (in other words a super-compressed detonation wave is realized). This lower limit of M , when η = = 0.1 , Q_3 = 100 kcal/mole , and Q_1 = 20 kcal/mole , equals 3.7 and with Q_1 = 35 kcal/mole , 2.8.

Proof of the Origin of a Plane Waveguide in the Reacting Gas Behind the Front of the Shock Wave

As shown above, the inversion layer can have a thickness on the order of 10 to 20 μ. With intensification of the light propagated along this layer, diffraction losses of photons occur, as well as losses associated with possible distortion of this layer. However, as we noted in [12], immediately behind the front of the shock wave there originates a thin layer of compressed gas with an elevated dielectric constant, ε . This layer can act as a plane waveguide for the intensified light. Compression occurs because with small x there takes place intense dissociation of original AX molecules (cf. (1) and curve 1 in fig 1) which draws off heat from the flow and reduces its temperature and speed. With great x , an exothermic recombination reaction takes place (cf. (3)), resulting in heating and acceleration of the flow and accordingly in a reduction in its density. With great x the density can be reduced to values lower than in the plane of x = 0 (cf., e.g., fig 3).

It has been assumed that a contribution to the real half of ε is made chiefly by a diluent gas in which there are no phototransitions in the region of the spectrum considered. Therefore below we disregard the variance of Re $\varepsilon(x)$ and assume that

$$\mathrm{Re}\,\varepsilon(x) = 1 + 2\beta\rho(x), \tag{13}$$

where β is a constant. In the waveguide having originated TE modes were calculated, whose electric field is determined by the equations

$$E_y = \mathcal{E}(x)e^{i(kz-\omega t)}, \quad \frac{d^2\mathcal{E}}{dx^2} + \left[\frac{\omega^2}{c^2}\mathrm{Re}\,\varepsilon(x) - k^2\right]\mathcal{E} = 0. \tag{14}$$

System of equations (4) to (10), (13) and (14) has been solved numerically with a computer; as a result the amplitudes of the lowest modes, $E^0(x)$, $E^1(x)$, etc., have been obtained. For β has been assumed a value corresponding to argon: $\beta = 0.08$ cm^3/g [15]; $\hbar\omega = 0.4Q_3$. The very existence of solutions for E(x) tending toward zero as $x \to \pm\infty$ proves the existence of the waveguide. It is obvious from fig 3 that the zero mode is localized in the inversion zone for this ω . The number of TE modes, N_ω , is finite. If $N_\omega \gg 1$, then it is determined from the equation

$$N_\omega = \frac{\omega}{\pi c} \int^{\infty} \sqrt{\mathrm{Re}\,(\varepsilon(x) - \varepsilon(\infty))}\, dx, \tag{15}$$

where the integral is taken for the region in which Re $(\varepsilon(x) - \varepsilon(\infty)) > 0$. For example, with the values of parameters indicated, but with $p_0 = 3$ atm, $N_\omega \simeq 60$.

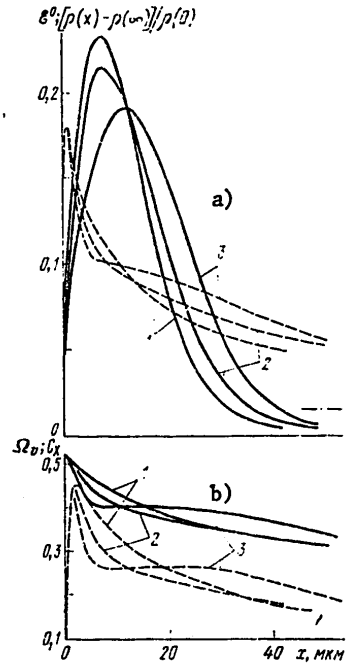

Figure 3. Spatial Dependences of E^0 (a, Straight Line), $[\rho(x) - \rho(\infty)]/\rho(0)$ (a, Dotted Line), Ω_v (b, Straight Line) and C_x (b, Dotted Line) for Values of Parameters in (11) with $\gamma/\gamma_p = 1$ (1), 0.7 (2) and 0 (3)

Key:
1. x, μ

In certain cases a waveguide originates also with an endothermic nonequilibrium reaction.

Light Gain in the Waveguide Mode

Let $I(z)$ be the integral flux of light energy for plane xy in this mode. Termed the light gain in this mode is the magnitude $\alpha = (1/I)dI/dz$. If $|\mathrm{Im}\,\varepsilon| \ll \mathrm{Re}\,(\varepsilon - 1)$, then

$$\alpha = -k\frac{\int_{-\infty}^{\infty} dx\,|\mathcal{E}(x)|^2\,\mathrm{Im}\,\varepsilon(x)}{\int_{-\infty}^{\infty} dx\,\mathrm{Re}\,\varepsilon(x)\,|\mathcal{E}(x)|^2} = \frac{\int_{-\infty}^{\infty} dx\,\alpha'(x)\,|\mathcal{E}(x)|^2}{\int_{-\infty}^{\infty} dx\,|\mathcal{E}(x)|^2}, \tag{16}$$

where

$$\alpha'(x) = a(\omega, T)\left\{[X]^2 - [X_2]K_3 e^{\frac{\hbar\omega}{kT}}\right\} - \tag{17}$$

is the light gain in an infinite spatially homogeneous mixture of gases; α' and $a(\omega,T)$ were computed in [4,6,16].

In disregarding laser generation, (16) corresponds to amplification of an extremely weak signal, $\alpha = \alpha_{sl\,[weak]}$, which was computed for the zero and first modes (cf. values of parameters in (11) and fig 3a): $\alpha_{sl} = 1.3\cdot10^{38}$ cm^{-6} and $-5\cdot10^{37}$ cm^{-6} for the zero and first modes respectively. Thus, the zero mode is intensified and the first damped.

Solution of Gas Dynamics and Kinetics Equations in the Presence of Laser Generation

In this case equations (4), (5), (7) and (14) and formulas (10), (13), (16) and (17) do not change. To the right half of (8) it is necessary to add the decrease in the number of atoms of X per unit volume per second on account of light-stimulated events of radiative chemical reaction (3): $-2W_{st}$, where

$$W_{ст}(x) = \frac{c\alpha'(x)}{\hbar\omega}U(x). \tag{18}$$

Here $U(x)$ is the integral density of electromagnetic energy in the waveguide for close frequencies of generated waves. To the right half of (9) it is necessary to add the increase in the number of molecules of X_2 per unit volume per second as the result of the same radiative reaction, i.e., W_{st}. To the left half of equation (6) it is necessary to add the term

$$\frac{\hbar\omega}{\rho_0 v_0}\int_0^{\lambda} dx\, W_{\text{ст}}(x),$$

associated with the energy going into radiation.

Then, in order for the system of equations to be complete, it is necessary to add also an equation determining the value of the steady-state energy content of the waveguide:

$$c\alpha = \gamma, \tag{19}$$

where γ is the energy decrement in the waveguide cavity resulting from various losses of photons, e.g., on account of the incomplete reflection of mirrors, which is assumed to be specified.

The self-consistent system of gas dynamics, kinetics and electrodynamics equations obtained in this way, in which $\varepsilon(x)$ depends on the concentration of gases and density, and the latter depend on the generated radiation, has been solved with a computer for different values of parameters.

In taking generation into account, i.e., terms with W_{st} and equations (19), to the parameters previously figured in the system of equations are added two new ones: $a(\omega,T)$ and γ. It is easy to see that the system of equations is invariant with a simultaneous substitution of $a \to \nu a$, $\gamma \to \nu\gamma$ and $U(x) \to U(x)/\nu$, where ν is an arbitrary number. Here the sought functions of x -- $[X]$, $[X_2]$ and other concentrations, $\rho(x)$, and also (with an accuracy of a constant factor) $E(x)$--remain unchanged. They depend, consequently, not on the two parameters a and γ, but only on the ratio of γ/a.

For the origin of generation it is necessary that the damping constant, γ, be below a certain threshold value of γ_p. The latter is chosen from the requirement that equation (19) be fulfilled with $U(x) \approx 0$, i.e., with $\alpha = \alpha_{s1}$. It is obvious that α_{s1}/a depends only on the previous parameters of the problem, but not on a and γ. Therefore, according to (19), $\gamma_p = c\alpha_{s1} = \alpha \cdot \text{const}$, where const depends only on the former parameters. Hence it follows that the solution can be tabulated as a dependence on parameter γ/γ_p (and not on γ/a).

As an example let us give the results of a calculation performed for values of the parameters in (11) and of $\hbar\omega = 0.4Q_3$. It is obvious from fig 3 that with a diminution in γ/γ_p there is an increase in the influence of stimulated radiation on kinetics and gas dynamics. Whereas for curves 1 and 3 the values of $\rho(\infty)$ agree, for curve 2, corresponding to the drawing off of energy from the flow, the value of $\rho(\infty)$ is greater (indicated by the dot-dash line in fig 3a). With a diminution in γ/γ_p the spatial behavior of density changes so that curve $E(x)$ becomes in form both lower and wider. The plateau on dotted-line curve 3 in fig 3b shows that in the region of $x = 20$ to 40 μ

C_X is greater with an evolved stimulated process than in its absence, although it would seem that stimulated radiation should annihilate atoms of X . This is explained by the fact that the inversion zone is located in the region of $X < 10$ μ and there C_X is actually lower than in the absence of stimulated radiation. In the region of $x = 20$ to 40 μ there is no inversion and the absorption of accumulated photons predominates, increasing C_X .

The power drawn off from 1 cm^2 of the stream on account of all kinds of losses of photons equals

$$\mathcal{P} = \gamma \int_{-\infty}^{\infty} U(x)\, dx. \qquad (20)$$

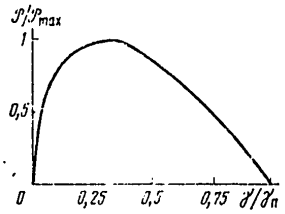

Figure 4. Dependence of P/P_{max} on γ/γ_p for Values of Parameters in (11)

If losses associated with the transmittance of the mirrors predominate, then P is the power of the generated laser radiation. In fig 4 is given the dependence of P on γ/γ_p with the values of parameters in (11). The maximum value of $P_{max} = 18.3$ kW/cm^2 is achieved with $\gamma/\gamma_p = 0.37$. Here from one gram of the gas mixture (including the diluent) an energy of 12.8 J is derived. It is obvious from fig 4 that when $\gamma \to 0$, $P \to 0$, unlike steady-state generation in a spatially homogeneous mixture of gases, where with a reduction in γ , beginning with the threshold value, P increases monotonically [2].

3. Investigation of Specific Chemiluminescent Mixtures Reacting According to System (1) to (3)

Having been selected are relatively stable initial compounds AX for which it is possible to disregard the reaction $AX + AX \to 2A + X_2$. In all cases the diluent was argon. Values of specific heat were taken from [17]. The equilibrium

constants, $K_1(T)$ and $K_3(T)$, for mixtures Nos 4 to 7, given in table 1, were also taken from [17]. For NOCl and NO_2Cl, K_1 was determined from the data in [18,19] and equaled respectively $3 \cdot 10^{25}$ exp $[-Q_1/(RT)]$ and $3.85 \cdot 10^{26}$ exp exp $[-Q_1/(RT)] \cdot (1500/T)^{3/2}$ cm^{-3}. For NOBr, K_1 was computed from the theoretical equation $K_1 = 5 \cdot 10^{25}$ exp $[-Q_1/(RT)]$ cm^{-3}, and Q_1 was taken from [20].

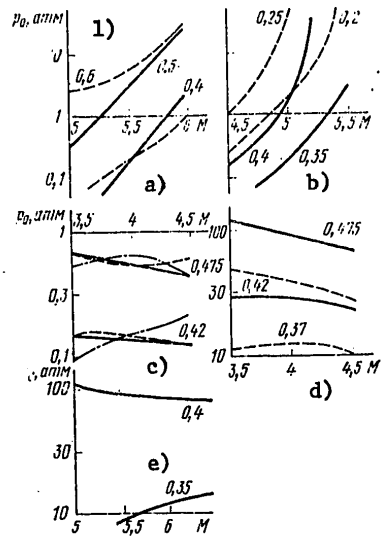

Figure 5. Maximum Values of Ω_v for Different P_0, M and η for Mixtures with Argon--O_3: $\eta = 0.1$ (straight line, a) and 0.2 (a, dotted line); N_2O: $\eta = 0.1$ (straight line, b); COS: $\eta = 0.01$ (b, dotted line); NO_2Cl: $\eta = 0.1$ (c, straight line), 0.5 (c, dotted line) and 0.2 (c, dash-dot line); NOBr: $\eta = 0.1$ (straight line, d); NOCl: $\eta = 0.1$ (d, dotted line) and NO_2: $\eta = 0.1$ (e); for the bottom dotted line in fig a, $\Omega_v = 0.5$

Key:

1. p_0, atm

In fig 5 are given the maximum values of function $\Omega_v(x)$ in relation to p_0 and M (similar to the oblique lines in fig 2). For the frequencies indicated with these curves inversion in the p_0, M plane is not achieved below the curves and is achieved (although in not too great a zone of x) in the plane above the curves.

Table 1. Parameters Used for Calculating Specific Substances

1) Номер смеси	X	A	2) E_1^0, ккал/моль	3) k_1^0, см³/(моль·с)	4) k_∞, с⁻¹	E_1^∞, ккал/моль
1	Cl	NO	34,79	$7,9\cdot10^{15}$ [24]	$1,7\cdot10^{11}$	34,79
2	Cl	NO_2	27,5	$6,3\cdot10^{16}$ [32]	$2,6\cdot10^{16}$	36,3 [31]
3	Br	NO	25,04	$1,1\cdot10^{15}$ [24]	$2,3\cdot10^{13}$	25,04
4	O	O_2	22,7	10^{15} [25]	$1,3\cdot10^{13}$	24,25 [23]
5	O	NO	65	$1,1\cdot10^{16}$ [23]	$2\cdot10^{14}$	72 [23]
6	O	N_2	58	$5\cdot10^{13}$	$1,3\cdot10^{11}$	59 [23]
7	S	CO	60,7	$1,5\cdot10^{14}$	$3,7\cdot10^{11}$	68,3 [23]

	k_2^0, см³/(моль·с)	E_2, ккал/моль	5) k_3, см⁶/(моль²·с)	Q_3, ккал/моль	6) $\lambda_{кр}$, мкм	7) $\Omega_{кр}$
1	$5,8\cdot10^{12}$	0 [30]	$1,4\cdot10^{14}$ [23]	58 [17]	1,3	0,38
2	$5,3\cdot10^{12}$	0	$1,4\cdot10^{14}$ [23]	58 [17]	1,3	0,38
3	$4\cdot10^{12}$	0	$2,9\cdot10^{14}$ [23]	46 [17]	1,5	0,41
4	$1,2\cdot10^{13}$	4,7 [25]	$2,5\cdot10^{13}$ [23]	120 [17]	0,6	0,4
5	10^{13}	0 [27]	$2,5\cdot10^{13}$ [23]	120 [17]	0,6	0,4
6	$3\cdot10^{13}$	25 [30]	$2,5\cdot10^{13}$ [23]	120 [17]	0,6	0,4
7	$6\cdot10^{13}$	27 [26]	$1\cdot10^{15}$ [28]	100 [17]	0,56	0,51

Note:

$$k_1=\left\{\left(k_1^0\right)^{-1}e^{E_1^0/RT}+([M]/k_\infty)\,e^{E_1^\infty/RT}\right\}^{-1};\quad k_3=k_2^0e^{-E_3/RT};$$

λ_{kr} is the red boundary of investigated wavelength regions for spontaneous chemiluminescence; $\Omega_{kr}=(h/\lambda_{kr})Q_3$.

[Key on following page]

Key:
1. Number of mixture
2. kcal/mole
3. $cm^3/(mole \cdot s)$
4. s
5. $cm^6/(mole^2 \cdot s)$
6. λ_{kr} , μ
7. Ω_{kr}

Fig 5 must be considered in comparison with the last column of table 1. For example, in the case of an O_3-Ar mixture (No 4 in table 1) luminescence is substantial in the spectrum region of $\Omega \geq 0.4$. To this mixture corresponds fig 5a, from which it is obvious that with this Ω in the case of thinning of $\eta = 0.1$ (solid-line curve) inversion is achieved already with a pressure of p_0 on the order of 1 atm and $M = 5.5$ to 6 , because of which the unit concentration of atomic oxygen, C_0 , is on the order of one. With $p_0 \approx 10$ atm , inversion exists also for shorter-wave radiation, right up to $\bar{\Omega} = 0.6$, i.e., $\lambda = 0.4$ μ .

A comparison of fig 5b to e with table 1 shows that in the case of mixture No 2 (fig 5c) inversion and high unit concentrations of atomic chlorine are also easily achieved. The situation is worse with the remaining mixtures. Mixtures Nos 6 and 7 are characterized by low velocity of reaction (1), since for them constant k_1^0 is very low. Therefore in situations when inversion is achieved in the necessary region of the spectrum C_X proves to be low. Mixtures Nos 1, 3 and 5 (fig 5d and e) achieve inversion in the necessary spectrum region only with high p_0 . We give the results of further calculations only for O_3 and NO_2Cl. Coefficient $a(\omega,T)$ figuring in (17), unlike in [16], was calculated on the assumption that with high pressures, because of the heavy impact broadening of luminescence lines, the rotational structure of spectra disappears. For a maximum of $a(\omega,T)$ the following values are obtained:

$$O+O,\ \lambda=0{,}6\ ,\ \mu\quad a=5\cdot10^{-41}(1000/T)^{3/2}\exp(-14{,}800/T)\ \text{см}^5;$$
$$Cl+Cl,\ \lambda=1{,}17\ ,\ \mu\quad a=2{,}4\cdot10^{-43}(1000/T)^{3/2}\exp(3300/T)\ \text{см}^5.$$

The gain for the waveguide mode was calculated from equations (16) and (17) for different values of p_0 and M . Unlike in sec 2, where a value of β was assumed corresponding to Ar, here and below were taken into account contributions to all $\mathrm{Re}\ \varepsilon$ of all components of the mixture, the polarizability of which was taken from [15]. Among calculated values for α_{s1} the following proved to be the highest:

$$\alpha_{сл}=1{,}5\cdot10^{-3}\ \text{см}^{-1}\quad \text{for}\quad O:Ar=1:5,\ p_0=17\ \text{атм},\ M=6{,}4. \tag{21}$$

$$\alpha_{сл}=3\cdot10^{-4}\ \text{см}^{-1}\quad \text{for}\quad NO_2Cl:Ar=1:20,\ p_0=8\ \text{атм},\ M=3{,}9. \tag{22}$$

Also obtained were dependences of P on γ/γ_p of the type given in fig 4. For the cases of (21) and (22), with $\gamma/\gamma_p = 1/3$, $P_{max} = 224$ and 8.7 kW/cm^2 , and the light energy obtained from 1 g of the mixture, 41 and 5.5 J, respectively.

4. Investigation of Specific Mixtures in Which Atoms Recombine Radiatively with Molecules of the Diluent

Let us consider the more complex reaction scheme in which in addition to (1) to (3) the following reactions take place:

$$M+X+M=MX+M+\begin{cases}\hbar\omega\\ Q\end{cases} \tag{23}$$

$$AX+M=A+MX, \tag{24}$$

$$X_2+M=MX+X. \tag{25}$$

The radiation channel important for laser generation is made possible now by reaction (23), and not by (3).

Instead of (8) and (9), in this case it is necessary to solve three kinetic equations, e.g., for [X], [X_2] and [MX]. W_{st} has the previous form in (18), but instead of (17) we get

$$\alpha'=\alpha(\omega, T)\{[X][M]-[MX]Ke^{\hbar\omega/kT}\}, \tag{26}$$

where K is the equilibrium constant of reaction (23). In a corresponding manner were changed the equations for the balance of matter and the expression for h in equation (6).

Below are considered five specific mixtures in which X is always an atom of hydrogen (Q_3 = 120 kcal/mole), and M and AX are given in table 2. The reaction rates of reactions (23) to (25) have a temperature dependence of the kind $k = k^0 \exp[-E^0/(RT)]$, and the values of k^0 and E^0 are given in table 3. The equilibrium constants for these reactions and other thermodynamic characteristics are taken from [17].

Inversion regions in which $\alpha' > 0$ are given in fig 6, similarly to fig 5. Mixture No 12 is not given in fig 6, since in the actual spectral region, according to calculation, inversion is not realizable for it. Mixture No 11 is unstable at room temperature; therefore for it was used a value of T_0 = = 100°K [21], whereas for the remaining mixtures in calculation it was assumed that T_0 = 300°K . Let us stress that if in figs 2, 5 and 6 along the X axis instead of M is plotted T immediately after the sudden shock (cf., e.g., fig 6b), then the curves maintain their position and form even for T_0 somewhat different from those established in calculations (strong shock waves). For all the mixtures given in fig 6 in the actual spectral region inversion is realizable at not too high pressures.

Table 2.

Номер смеси 1)	M	ΔX	$\lambda_{кр}$, мкм 2)	$\Omega_{кр}$ 3)
8	CO	O_3	0,8	0,3
9	CO	N_2O		
10	CO	NO_2		
11	NO	O_3	1,4	0,17
12	NO	NO_2		

Key:
1. Number of Mixture
2. λ_{kr}, μ
3. Ω_{kr}

Table 3.

Реакция 1)	k^*	2) E^*, ккал/моль	3) Литература
$O_3 + CO$	$6 \cdot 10^{11}$	22	[29]
$N_2O + CO$	$1,1 \cdot 10^{11}$	23	[5]
$NO_2 + CO$	$2 \cdot 10^{12}$	29	[5]
$O_3 + NO$	$4,2 \cdot 10^{12}$	23	[21]
$N_2O + NO$	$2,5 \cdot 10^{13}$	50	[5]
$O_2 + CO$	$3 \cdot 10^{12}$	51	[30]
$CO + O + M$	$6,2 \cdot 10^{13}$	0	[30]
$NO + O + M$	$8 \cdot 10^{11}$	0	[27]

Note: The reaction rates of bimolecular reactions are given in $cm^3/(mole \cdot s)$, and of trimolecular, in $cm^6/(mole^2 \cdot s)$.

[Key on following page]

Key:
1. Reaction
2. kcal/mole
3. Bibliography

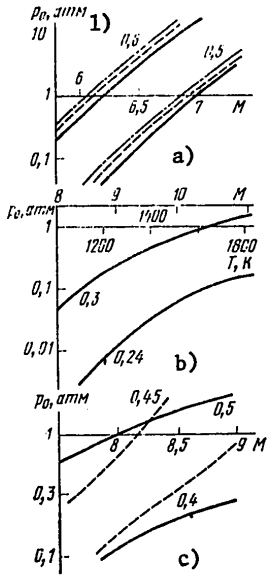

Figure 6. Maximum Values of Ω_v for the Following Mixtures: O_3-CO: η = 0.1 (solid line); 0.05 (dotted line) and 0.025 (dot-dash line) (a); O_3-NO (b); NO_2-CO (solid line) and N_2O-CO (c, dotted line); for b and c, η = 0.01

Key:
1. p_0, atm

In order to give preference to one of these mixtures it is necessary to consider characteristics of them not given in fig 6. In particular, important are the values of gain in which totally taken into account are concentrations of atomic oxygen, the properties of the waveguide, etc. Gain was computed for many values of p_0 and M. In all cases it was assumed that $\eta = 0.1$. The following maximum values of α_{s1} were obtained for the zero waveguide mode:

$$\alpha_{сл}=1{,}2\cdot 10^{-3}\ \text{см}^{-1} \quad \text{for} \quad O_3\text{—CO},\ p_0=12\ \text{атм},\ M=6,$$

$$\begin{aligned}
&\alpha_{сл}=4\cdot10^{-5}\ \text{см}^{-1} \quad \text{for} \quad N_2O\text{—}CO,\ p_0=7\ \text{атм},\ M=7{,}6,\\
&\alpha_{сл}=2\cdot10^{-4}\ \text{см}^{-1} \quad \text{for} \quad NO_2\text{—}CO,\ p_0=13\ \text{атм},\ M=7{,}4,\\
&\alpha_{сл}=3\cdot10^{-5}\ \text{см}^{-1} \quad \text{for} \quad O_3\text{—}NO,\ p_0=0{,}1\ \text{атм},\ M=8{,}5.
\end{aligned} \tag{27}$$

In the case of the last mixture were studied only pressures not greater than 0.1 atm, since for $T_0 = 100°K$ with great pressures the mixture is condensed. It is obvious from the data given that α_{sl} is maximum for a mixture of O_3-CO.

It is obvious from the results of secs 3 and 4 that O_3 is a better donor of atomic oxygen than N_2O and NO_2. This is associated with the fact that in O_3 the activation energy for separation of an oxygen atom, E_1^0 is less than in the other molecules studied, and pre-exponential factor k_1^0 is fairly high (cf. table 1).

For a mixture of O_3:CO = 1:10 and for the parameters in (27) the equations were solved by taking into account the stimulated radiation. Arrived at were $P = 155\ kW/cm^2$ with $\gamma/\gamma_p = 0.22$, and the light energy equals 54 J from one gram of the mixture. This value of P is not, generally speaking, the maximum possible, since in this and the previous sections we selected p_0 and M so that α_{sl} would be maximum, and not P_{max}.

We were convinced that in all the cases considered M corresponds to conditions of supercompressed detonation, when steady-state flows with a shock wave exist [13]. Checked also was the test for the stability of unidimensionality of the flow (of a plane front) [22]. A plane front of supercompressed detonation can be accomplished either by means of a piston pushing the studied gas at supersonic speed, as is done in a shock tube, or in a supersonic steady-state flow of this gas. The velocity of the flow and its variable cross section can be selected so that the front of the shock wave will be stationary.

The radius of curvature, caused by viscous layers near the walls, of the front of a shock wave traveling through a tube 10 cm in diameter equals $R \gtrsim 100$ m. At the same time losses of photons resulting from distortion of the waveguide's plane become comparable with the calculated values of α only with R on the order of a few centimeters. Because of the origin of a waveguide it is possible to accomplish feedback in a laser without mirrors, when in a non-unidimensional flow the front of the shock wave, the waveguide and the path of the light beam form a closed circuit.

According to estimates, with evolved generation in a waveguide the strength of the electric field can reach a value on the order of 10 MV/cm, which creates the threat of a breakdown of gas even at frequencies corresponding to visible light.

Conclusion

With the example of specific gas mixtures it has been shown that by means of a shock wave it is possible to trigger an electron transition chemical laser with high flow density and speed, i.e., with high supplied chemical power. A proof has been given of the possibility of the formation of a plane waveguide behind the front of the shock wave, which eliminates losses of light associated with slight thickness of the generation layer. The conditions for formation of the waveguide are compatible with conditions for the origin of inversion and intensification. For the types of reactions considered the positive role of the diluent consists in acceleration of the useful reaction for the dissociation of donors of X atoms, making it possible for this reaction to compensate the consequences of harmful reactions which destroy X atoms. Pumping of these lasers is accomplished on account of chemical and mechanical energy of the gas flow comparable in magnitude. For specific gas mixtures a gain on the order of 10^{-3} cm^{-1} has been achieved and a power on the order of 100 kW/cm^2 of the cross section of the gas flow, which exceeds the unit power of all known chemical and thermal lasers.

Bibliography

1. Pekar, S.I. DAN SSSR, 187, 555 (1969).

2. Kochelap, V.A. and Pekar, S.I. ZHETF, 58, 854 (1970); UFZH, 15, 1057 (1970).

3. Kochelap, V.A. and Pekar, S.I. DAN SSSR, 196, 808 (1971).

4. Kochelap, V.A., Kukibnyy, Yu.A. and Pekar, S.I. KVANTOVAYA ELEKTRONIKA, 1, 279 (1974).

5. Tal'roze, V.L., Gordon, Ye.B., Moskvin, Yu.L. and Kharitonov, L.P., DAN SSSR, 214, 846 (1974).

6. Bashkin, A.S., Igoshin, V.I., Nikitin, A.N. and Orayevskiy, A.N. "Khimicheskiye lazery" [Chemical Lasers], Moscow, VINITI, 1975.

7. Biryukov, A.S., Prokhorov, A.M., Shelepin, L.A. and Shirokov, N.N., ZHETF, 67, 2064 (1974).

8. Losev, S.A. "Gazodinamicheskiye lazery" [Gas Dynamical Lasers], Moscow, Nauka, 1977.

9. "Electronic Transition Lasers" in "Proc. 2nd Summer Colloq., Woods Hole, Sept. 17-19, 1975."

10. Ekstrom, D.J., Barker, J.R., Hawley, J.G. and Reilly, J.P. APPL. OPTICS, 16, 2102 (1977).

11. Gross, R.W.F., Giedt, R.R. and Jacobs, T.A. J. CHEM. PHYS, 51, 1250 (1969).

12. Pekar, S.I., Izmaylov, I.A., Kochelap, V.A. and Kukibnyy, Yu.A. DAN SSSR, 241, 80 (1978).

13. Zel'dovich, Ya.B. and Rayzer, Yu.P. "Fizika udarnykh voln i vysokotemperaturnykh gazodinamicheskikh yavleniy" [Physics of Shock Waves and High-Temperature Gas Dynamical Phenomena], Moscow, Nauka, 1966.

14. Kondrat'yev, V.N. and Nikitin, Ye.Ye. "Kinetika i mekhanizm gazofaznykh reaktsiy" [Kinetics and Mechanism of Gas Phase Reactions], Moscow, Nauka, 1974.

15. "Tablitsy fizicheskikh velichin" [Tables of Physical Magnitudes], edited by I.K. Kikoin, Moscow, Atomizdat, 1976.

16. Izmaylov, I.A., Kochelap, V.A. and Kukibnyy, Yu.A. UFZH, 21, 508 (1976).

17. Glushko, V.M. "Termodinamicheskiye svoystva individual'nykh veshchestv" [Thermodynamic Properties of Individual Substances], Moscow, Izdatel'stvo AN SSSR, 1962.

18. Ashmore, P.J. and Spencer, M.S. TRANS. FARADAY SOC., 55, 1868 (1959).

19. Ashmore, P.J. and Burnett, M.J. TRANS. FARADAY SOC., 57, 1315 (1961).

20. "Energiya razryva khimicheskikh svyazey. Potentialy ionizatsii i srodstvo k elektronu" [Energy of Breaking of Chemical Bonds; Ionization Potentials and Electron Affinity], edited by V.N. Kondrat'yev, Moscow, Mir, 1974.

21. Izmaylov, I.A., Kochelap, V.A. and Kukibnyy, Yu.A. In the collection "Kvantovaya Elektronika" [Quantum Electronics], Kiev, Naukova Dumka, No 14, 1976, p 26.

22. Shchelkin, K.I. and Troshin, Ya.K. "Gazodinamika goreniya" [Gas Dynamics of Combustion], Moscow, Izdatel'stvo AN SSSR, 1963.

23. "Fizicheskaya khimiya bystrykh reaktsiy" [Physical Chemistry of Fast Reactions], edited by I.S. Zaslonko, Moscow, Mir, 1976.

24. Maloney, K.K. and Palmer, H.B. INT. J. CHEM. KINET., 5, 1023 (1973).

25. Center, R.E. and Kung, R.T. J. CHEM. PHYS., 62, 802 (1975).

26. Hay, A.J. and Belford, R.L. J. CHEM. PHYS., 47, 3944 (1967).

27. Dushin, V.K. and Losev, S.A. NAUCHNYYE TRUDY NII MEKHANIKI MGU, No 43, 102 (1976).

28. Thrush, B.A. and Fair, R.W. DISC. FARADAY SOC., 44, 237 (1967).

29. Garvin, D. J. AMER. CHEM. SOC., 76, 1523 (1954).

30. Kondrat'yev, V.N. "Konstanty skorosti gazofaznykh reaktsiy" [Reaction Rates of Gas Phase Reactions], Moscow, Nauka, 1971.

31. Martin, H. and Knauth, H.D. BER. BUNSENGES PHYS. CHEM., 73, 922 (1969).

32. Cordes, H.F. and Jonston, H.S. J. AMER. CHEM. SOC., 76, 4264 (1954).

CSO: 1862
8831

LASERS AND MASERS

UDC 621.373.8.537.533

OPTIMIZATION OF ELECTRON BEAM PARAMETERS AND CHOICE OF FOIL IN ELECTRON BEAM CONTROLLED LASERS

Moscow KVANTOVAYA ELEKTRONIKA in Russian Vol 6 No 8, Aug 79 pp 1690-1697
manuscript received 20 Nov 78

[Article by A.I. Dutov, S.V. Minayev and V.B. Nikolayev]

[Text] By the Monte Carlo method a study was made of the transmission of relativistic electrons through the foil-gas-anode system in an electron beam controlled laser (EIL). The influence is discussed of beam parameters, the composition of the active medium and the electric field in semi-self-maintained discharge, as well as of the design features of the laser on homogeneity of ionization in the discharge gap and on uniformity of the electric field in it. Questions are discussed relating to selection of the beam's energy and design elements of the laser when using light foils.

1. Introduction

In an electron beam controlled laser the electron beam, accelerated to relativistic velocities, passes through a vacuum-type foil and ionizes the active medium, which makes it possible to contribute considerable energy to large volumes of the active material [1,2]. At the present time considerable attention is being devoted to problems of spatial homogeneity and stability of a semi-self-maintained discharge in laser mixtures [3-6]. A number of authors have noted that nonuniformity of ionization over the cross section and length of the discharge gap contributes to instability of the discharge [4,5,7,8]. Obviously associated also with inhomogeneous ionization of the laser cavity and with subsequent nonuniform excitation are inhomogeneities in gain and in the final analysis in the medium's refractive index [9]. The limiting characteristics of an EIL of both the continuous and pulsed periodic type depend not only on these factors, but also on the heat resistance and transmitting capacity of foils [10].

These problems are responsible for the considerable interest in investigations of the transmission of electron beams through foils and active media in EIL's. In addition, in the majority of studies on the theoretical plane important factors influencing the pattern of the process have not been taken into account. For example, in some studies the electron beam on its entrance into

the gas was considered monochromatic, i,e,, the consequences of scattering of electrons in the foil were not taken into account [13]. In studies [5,13] the distribution of ionization losses in laser mixtures was studied only with nitrogen as an example. Often not paid attention to has been the presence of the anode of the primary discharge, although it is known that electrons reflected back can effectively ionize part of the gap [12]. It is also necessary to take into account the structural arrangement of the cathode, usually executed in the form of a grid, since there is no electric field between the foil and cathode. This exerts an influence on formation of energy and angular distributions in the flow of electrons arriving at the cathode. An investigation of laser construction has been made in just one study [12]. Here a study was made of the influence of the anode's material on the distribution of ionization losses in the gap, but calculations were made only for a single specific combination of parameters.

In this paper a study is made of the transmission of electrons with energy of 100 to 250 keV through the foil-gas-anode system in an EIL and an estimate is made of homogeneity in ionization of the working material in relation to the height of the discharge gap. Discussed are standard foils, typical laser mixtures at atmospheric pressure and electric fields in a semi-self-maintained discharge. Of course, the energy and angular spectra of relativistic electrons depend on the type of electron gun; in particular, for systems with a field emitter the energy spectrum is of a rather complex nature, which together with broad angular distribution results in considerable losses in passing through the foil [15]. Pulsed powering of an electron gun with a cathode of any type also results in added losses in the foil as compared with a gun operating with a steady power supply. Therefore in our calculations it was assumed that in the EIL is employed a grid-controlled electron gun operating with a steady acceleration voltage [16,17] and making possible monochromaticity of electrons and orthogonalization of their paths to the emitting foil window.

In this study are calculated distributions of ionization losses, $D(x)$, and of the electric field, $E(x)$, over the height of the discharge gap. Furthermore, the energy of the monochromatic electron beam, E_0 , hitting the foil was varied, as was also the magnitude of the electric field, E_x , averaged in terms of the length of the discharge, and applied between the cathode grid and anode. A study is made of the influence of the thickness and material of the foil, as well as of the composition of the active medium and of the anode's material, on these distributions. The calculations made make it possible to draw certain conclusions regarding optimization of the parameters of electron beams and foils, as well as to specify requirements for the design of EIL's.

2. Calculation Procedure

These distributions and characteristics were calculated by the Monte Carlo method with reference to a model of continuous deceleration [18]. In each case were considered the paths of travel of not less than $2 \cdot 10^3$ electrons hitting the foil. Here mean ionization losses per unit length of the electron's path in the material of the foil and of the laser medium were determined from Bethe's equation, and the angular distribution of electrons was calculated

with Molière's equations [18]. The thickness of the Molière layer was chosen so that 20 to 25 collisions would occur in it. Consideration of the three-dimensional motion of an electron in the medium ceased when its energy dropped to 10 keV. Let us note that for the purpose of reducing the calculation time it is possible to consider the two-dimensional path of an electron. An analysis has shown that here acccuracy is reduced five percent in calculating the transmission of foils [19] and 10 to 15 percent in calculating losses in the gas.

The original electric field in the discharge gap was considered homogeneous and constant at the initial stage of the discharge. In all figures, except specially stipulated cases, the foil is located in plane $x = 0$, and the cathode grid with 100 percent transmittance, in plane $x = 2$ cm . Based on distributions of losses, $D(x)$, obtained in the foil-gas-anode system, the function of the secondary electron source was computed, i.e., the rate of formation of electron-ion pairs in the gap [20]. Then, according to a procedure similar to [7], were calculated local changes in the electric field, $E(x)$, in the discharge gap. The cathode drop was not taken into account, since in a typical EIL its spatial spread equals approximately 10^{-2} to 10^{-4} cm [21]. For a mixture of CO_2:N_2:He = 1:2:3, the distribution of $E(x)$ was calculated by taking into account the dependence of the recombination coefficient on the electric field [22].

For the purpose of checking the correctness of the procedure, variants were calculated, data on which were available in the literature. The discrepancy with the results of studies [10-12, 14, 23] proved to be less than 10 percent.

3. Results of Calculations

In figs 1 and 2 are given unidimensional distributions of ionization losses, $D(x)$, in keV/cm, over the length of the discharge gap taking into account different factors influencing the homogeneity of ionization. Here it was assumed that the anode is an ideal absorber of electrons, which made it possible to isolate its influence from other effects. In fig 1 are shown distributions for four values of the energy of the electron beam, E_0 , hitting an aluminum foil 25 μ thick (curves 1 to 4). From this figure it is possible to estimate to what extent the degree of homogeneity of ionization depends on the length of the gap selected for each energy value. For example, at a distance of 10 cm from the cathode the decline in ionization relative to the maximum equals 38, 20 and 10 percent for beams with energy of 130, 150 and 200 keV, respectively. At a distance of 18 cm from the cathode for these same energies the decline in ionization reached 66, 40 and 30 percent (and only seven percent for E_0 = 250 keV). Calculation of similar relationships with a foil thickness of 50 μ showed that the value of the ionization maximum was reduced for low E_0 and grew for high. The homogeneity of ionization worsened considerably, especially for beams with energy of 130 and 150 keV, for which the mean free path of electrons was drastically shortened.

Curves 1 to 4 (fig 1) relate to the typical laser mixture CO_2:N_2:He = 1:2:3, which is relatively light because of its strong helium content. In working

with more inexpensive He-free mixtures it is necessary to take into account their strong retarding capacity. Curves 5 and 6 (fig 1) show the behavior of the dependence of ionization losses, D(x) , for nitrogen and the mixture CO_2:N_2 = 1:3, respectively, with E_0 = 150 keV . Obviously, in changing to denser gases is observed a sudden increase in the degree of ionization, as well as in inhomogeneity (cf. curves 2, 5 and 6 in fig 1).

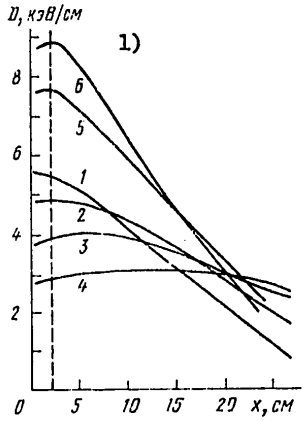

Figure 1. Distribution of Ionization Losses Over the Length of the Gap with E_x = 5 kV/cm for Mixtures of CO_2:N_2:He = 1:2:3 (1 to 4), CO_2:N_2 = 1:3 (6) and for Pure Nitrogen (5); E_0 = 130 (1), 150 (2,5,6), 200 (3) and 250 keV (4)

Key:
1. D, keV/cm

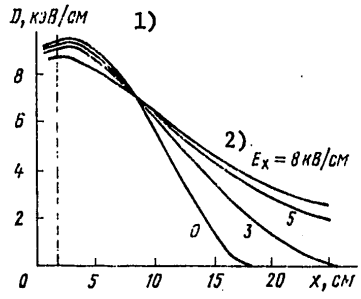

Figure 2. Distribution of Ionization Losses Over the Length of the Gap as a Function of the Electric Field for the Mixture CO_2:He = 1:3

[Key on following page]

Key:
1. D, keV/cm
2. E_x = 8 kV/cm

As early as in the first study on the calculation of losses [14] it was noted that it is necessary to take into account the influence of the electric field on the travel of electrons in the gap. In fig 2 are shown distributions of losses, D(x) , in taking into account several typical values of the electric field, E_x (E_0 = 150 keV , aluminum foil 25 μ thick). Obviously, an electric field applied collinearly to the direction of travel of electrons considerably extends the mean free path of electrons in the gas, but the magnitude of the field has a but slight influence on the degree of inhomogeneity in ionization of a gap 10 to 15 cm long. It is significant that curves for E_x = 5 and 8 kV/cm are very close in the gap considered.

For the purpose of approximation to a real EIL system, calculations were made by taking into account electrons repelled from the anode. In fig 3 are shown dependences of losses D(x) and fields E(x) for two specific laser units described in [16]. In both cases were used identical acceleration voltages (E_0 = 150 keV), foils and discharge gaps. The difference consisted in the composition of the gas mixture and the strength of the electric field in the discharge. Obviously for the mixture CO_2:N_2 = 1:3 there is a considerable decline in ionization near the anode (approximately 50 percent), and electrons repelled by an aluminum anode improve homogeneity but slightly. The distribution of the electric field in this case is strikingly inhomogeneous. For the light mixture CO_2:N_2:He = 1:2:3, the homogeneity of ionization is fairly high (approximately five percent) and the role of the anode in equalizing ionization and the electric field is substantial. From comparing figs 3a and b it becomes understandable why in the case of a light mixture in the experiment it was possible to realize a higher energy contribution and energy output in spite of the great difference in electric fields in favor of the heavy mixture [16]. With an increase in the beam energy, E_0 , to 200 keV, the contribution of electrons repelled from the anode to ionization of the gap can have a considerable influence not only on homogeneity, but also on the degree of ionization (fig 4). In the same figure it is shown that with an increase in density and atomic number of the anode's material the share of repelled electrons in ionization grows and reaches 50 percent at the anode, which is in agreement with the results of study [12].

A role of no slight importance in the interaction of an electron flow with an active gaseous medium is played by the energy and angular distributions of electrons formed after the beam passes through the foil. We calculated the energy and angular spectra for beams with an initial energy of E_0 = 150 keV , having passed through various foils. It is obvious from fig 5 that foils with low unit density differ advantageously from heavier foils in the sense of preserving the monochromaticity and directivity of the beam. Especially distinguished is a Lavsan film.

The distributions of ionization losses, D(x) , given in figs 1 to 3 were obtained on the basis of a single electron hitting the foil. For the purpose of estimating the function of the secondary electron source and the distribution

of the concentration of electrons in the discharge gap this is sufficient, but for the purpose of calculating heat release in foils also required is knowledge of energy losses per single electron in passing through the film. The table gives an idea of the transmission coefficients of standard foils in relation to energy, T_E, and current, T_N, on the assumption of monochromaticity of the electron beam and normal incidence on the foil. Calculations for current agree well with experimental study [23], and for coefficients T_N and T_E, with theoretical study [11] (with an accuracy of one percent). There is also agreement with the results of studies [12,14], if it is taken into account that contributing to coefficient T_E are both ionization losses of the primary beam and the energy of electrons repelled from the foil. Actually, in the final analysis repelled electrons basically return to the foil and are absorbed in it because of the braking field of the electron beam. Also indicated in the table are calculated values of the mean scattering angle, $\bar{\alpha}$, and the mean energy of an electron, $\bar{E}$, passing through the foil. Thus, the table supplements fig 5.

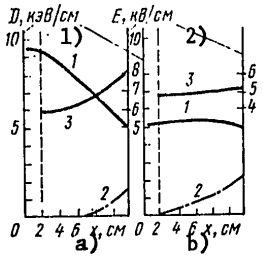

Figure 3. Distribution of Ionization Losses (1) and Electric Field Strength (3) in the Discharge Gap According to the Data of [16], as Well as Contribution to Ionization of Electrons Repelled from the Anode (2) for Mixtures of CO_2:N_2 = 1:3 with E_x = 6.6 kV/cm (a) and CO_2:N_2:He = 1:2:3 with E_x = = 4 kV/cm (b)

Key:
1. D, keV/cm
2. E, kV/cm

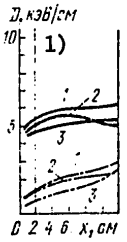

Figure 4. Distribution of Ionization Losses, D(x), in the Discharge Gap (Solid Lines) and Contribution to Ionization of Electrons

[Caption continuation and key on following page]

Repelled from the Anode (Dot-Dash Lines) for Anodes Made of Copper (1), Steel (2) and Aluminum (3); E_0 = 200 keV ; Foil, Aluminum, 25 μ Thick; Mixture of CO_2:N_2:He = 1:2:3; E = 5 kV/cm

Key:
1. D, keV/cm

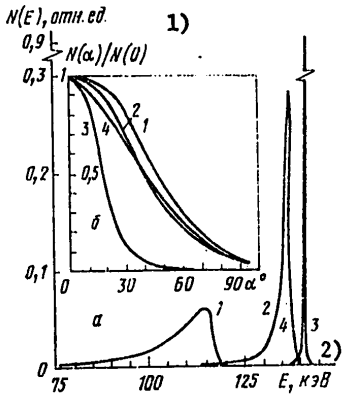

Figure 5. Energy (a) and Angular (b) Spectra of Electrons Having Passed Through Foils of Different Thickness: 1--aluminum, 50 μ ; 2--aluminum, 25 μ ; 3-- Lavsan, 20 μ ; 4--titanium, 13 μ

Key:
1. N(E) , relative units 2. E , keV

4. Discussion of Results and Optimization of Unit

The calculation routines which have been developed make it possible to select the optimal energy of the primary beam with a specified set of parameters: the material and thickness of the foil, the composition of the mixture, the length of the discharge gap and the strength of the electric field in it. For example, for an EIL with a discharge gap approximately 20 cm long and an aluminum foil 25 μ thick, increasing the energy of the beam, E_0 , about 150 keV is not advisable in the case of light mixtures. Calculations which we have made showed that increasing the energy of the beam by 50 keV, other conditions being equal, practically does not change the level of ionization in the gap and even slightly worsens homogeneity. It was indicated in [2] that increasing the energy of the beam higher than 150 keV did not result in the experiment in a noticeable increase in contributions of energy to the discharge. With a further increase in beam energy there will be an increase

in the share going into heat and x-radiation in the primary discharge anode, and the mean free path of repelled electrons will also be increased. Consequently, ionization near the anode will grow, which can result in strengthening of the field near the cathode and in the appearance there of discharge instability.

Table

1) Тип фольги	Толщина, мкм 5)	ρ, мг/см² 6)	E_0, кэВ 7)	T_N, %	T_E, %	$\bar{\varphi}$, рад 8)	$\bar{E}$, кэВ
Алюминий 2)	50	13,7	150 200	62 85	40 67	0,79 0,76	96 157
Алюминий	25	6,85	150 200	91 96	77 88	0,72 0,61	128 183
Титан 3)	20	9,0	150 200	74 88	57 77	0,81 0,76	116 175
Титан	13	5,65	150 200	88 95	77 88	0,77 0,67	131 186
Лавсан 4)	20	2,8	100 150	98 99(,7)	87 94	0,56 0,41	88 142

Key:

1. Type of foil
2. Aluminum
3. Titanium
4. Lavsan
5. Thickness, μ
6. mg/cm^2
7. keV
8. Radians

Of no slight importance also is the fact that with an increase in acceleration voltage the high-voltage power supply of the gun becomes complicated and the requirements for its insulation are increased, the biological shield becomes heavier in proportion to the energy and the like, i.e., the cost of the unit increases and its reliability is reduced.

On the other hand, reduction of the electron beam's energy is advantageous only to a specific limit, related basically to the foil chosen. Actually it is important to ensure low losses in the foil, as well as to form behind the foil the required energy and angular distribution in the beam (cf. table and fig 5). Then by proper selection of the position and material of the anode it is possible to compensate the natural decline in ionization in the gap.

An optimal material for the outlet window is obviously polymer films, e.g., Lavsan. Actually, it is obvious from the table that the transmission coefficients of aluminum foil 25 μ thick and of titanium 13 μ thick for E_0 = 200 keV are very close to the transmission coefficient of a Lavsan film 20 μ thick

as soon as $E_0 \approx 100$ keV . This is sufficient for ensuring insignificant heat release in the film.

It is obvious from the table that in changing from aluminum foil 50 μ thick to a Lavsan film 20 μ thick the transmission of energy for $E_0 = 150$ keV increases from 40 to 94 percent, and the transmission in terms of number of particles from 62 to almost 100 percent. For a laser of the continuous or pulsed periodic type this substantial difference in transmitting capacity of light and heavy foils is intensified more so by the fact that in a real electro-optical system of a gun it is impossible to count on the fact that the paths of all electrons striking the foil will be orthogonal to it. This results [19] in drastic worsening of the transmission of foils with angles of incidence of electrons approximately greater than 60 degrees, which in turn entails an increase in heat release in the foil and can cause additional inhomogeneities in ionization in the gap.

Let us consider a few examples of optimizing the energy of the electron beam and the parameters of the discharge gap on the basis of using a Lavsan film 20 μ thick and of an assigned value of the mean electric field in the gap of 5 kV/cm. In fig 6 are shown the distributions of ionization losses and the electric field in a discharge gap 20 cm long for the mixture $CO_2:N_2:He$ = = 1:2:3. Homogeneity in ionization at a level of a few percent (curve 1) is achieved here by employing an acceleration voltage of E = 150 kV , as well as by drawing the cathode grid 4 cm back from the foil. From fig 6 it is obvious what an important role is played by electrons repelled from a steel anode (curve 3).

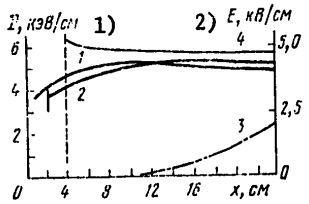

Figure 6. Distribution of Ionization Losses (1,2) and Electric Field (4) in the Discharge Gap for a Cathode Grid Distance of 4 cm (1,4) and 2 cm (2): 3--Contribution to Ionization of Electrons Repelled from a Steel Anode

Key:
1. keV/cm
2. kV/cm

For a gap 10 cm long the optimal calculated beam energy is $E_0 \approx 110$ keV for the same mixture and anode material, but here changing the beam energy a total of $\pm$ 10 keV resulted in a decrease in ionization at the anode or cathode of 30 percent.

With the same design parameters of the EIL, for the purpose of achieving homogeneous ionization in heavy mixtures, e.g., CO_2:N_2 = 1:3, it is necessary to deal with higher beam energies. In fig 7 is shown an example of achieving uniformity in the absorbed dose by selecting the acceleration voltage (E_0 = 180 to 200 keV) and position of the cathode grid. It is obvious that in this manner it is possible to achieve a reduction in homogeneity of approximately 15 percent (curve 2). For a discharge gap 10 cm long with the same mixture an optimal beam energy of E_0 = 150 keV was obtained with a cathode-to-foil distance of 3 cm. Varying this distance over a range of $\pm$ 1 cm resulted in a decrease in ionization near electrodes of 20 percent.

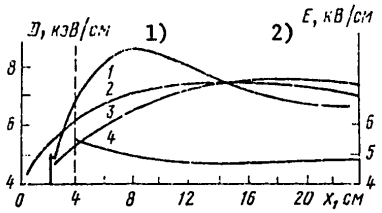

Figure 7. Distribution of Ionization Losses (1-3) and Electric Field (4) in a 20 cm Gap for E_0 = 180 keV and a Cathode Grid Distance of 2 cm (1), 200 keV and 3 cm (2,4) and 200 keV and 2 cm (3)

Key:
1. keV/cm
2. kV/cm

Calculations made with discharge gaps 30 cm long when using aluminum foil 25 μ thick demonstrated that it is possible to achieve uniformity in ionization on the order of 10 percent with a beam energy of E_0 = 250 keV both for light and for heavy mixtures. Here the decisive role in the formation of ionization near the cathode is played by the position of the cathode grid, and in equalization of the absorbed dose at the anode, by the material of the anode.

Thus, the utilization of light foils with a simultaneous reduction of the energy of the electron beam makes it possible to increase the concentration of secondary electrons in the plasma, to reduce the cross section of the discharge (because of a reduction in scattering angles in the foil), as well as to facilitate the biological shield and to simplify the unit. Light foils are distinguished also by reduced losses with respect to energy and the number of particles, which makes possible the transmission by them of greater mean power of the electron flow. In the literature there is information also regarding the employment of an aluminum foil 12 μ thick in a pulsed CO_2 laser [22] and of a synthetic film of the same thickness in a continuous production process laser [24], which testifies to the surmountability of the technical difficulties associated with compacting thin foils and removing heat.

In operation under optimal conditions it is necessary also to keep in mind that if during the period of a pulse the beam energy varies by a total of 10 to 20 keV this can result in redistribution of ionization losses over the discharge gap and in intensification of the electric field in the cathode or anode region.

In conclusion the authors wish to express their thanks to A.A. Mak for his helpful discussions and to Yu.A. Anan'yev and N.N. Rozanov for their constant attention and assistance in this paper.

Bibliography

1. Basov, N.G., Belenov, E.M., Danilychev, V.A. and Suchkov, A.F. UFN, 114, 213 (1974).

2. Danilychev, V.A., Kerimov, O.M. and Kovsh, I.B. TRUDY FIAN, 85, 49 (1976).

3. Boer, K., Henderson, D.B. and Morse, R.L. J. APPL. PHYS., 44, 5511 (1973).

4. Yevdokimov, O.B., Mesyats, G.A. and Ponomarev, V.B. FIZIKA PLAZMY, 3, 357 (1977).

5. Yevdokimov, O.B., Ryzhov, V.V. and Yalovets, A.P. ZHTF, 47, 2517 (1977).

6. Theophanis, G.A., Jacob, J.H. and Sackett, S.J. J. APPL. PHYS., 46, 2329 (1975).

7. Jacob, J.H., Reilly, J.P. and Pugh, E.R. J. APPL. PHYS., 45, 2609 (1974).

8. Bychkov, Yu.I., Genkin, S.A., Korolev, Yu.D., Mesyats, G.A., Rabotkin, V.G. and Filonov, A.G. IZVESTIYA VUZOV SSSR, SERIYA FIZIKA, No 11, 139 (1975).

9. Pugh, E.R., Wallace, J., Jacob, J.H., Northam, D.B. and Daugherty, J.D. APPL. OPTICS, 13, 2512 (1974).

10. Denholm, A.S. and Quintal, B.S. LASER FOCUS, 10, No 7, 41 (1974).

11. Seltziar, S.M. and Berger, M.J. NUCL. INSTR. AND METH., 119, 157 (1974).

12. Smith, R.C. APPL. PHYS. LETTERS, 25, 292 (1974).

13. Yevdokimov, O.B. and Yalovets, A.P. ZHTF, 44, 217 (1974).

14. Smith, R.C. APPL. PHYS. LETTS., 21, 352 (1972).

15. Ahlstrom, H.G., Inglesakis, G., Holzichter, J.F., Kan, T., Jenson, J. and Kolb, A.C. APPL. PHYS. LETTS., 21, 492 (1972).

16. Avanesyan, V.S., Dutov, A.I., Lakhno, Yu.V. and Malakhov, L.N. KVANTOVAYA ELEKTRONIKA, 4, 1827 (1977).

17. Dutov, A.I. and Nikolayev, V.B. "Tezisy dokladov I Vsesoyuz. konf. 'Optika lazerov'" [Theses of Papers at the First All-Union "Optics of Lasers" Conference], Leningrad, GOI, 1977, p 108.

18. Baranov, V.F. "Dozimetriya elektronnogo izlucheniya" [Electronic Radiation Dosimetry], Moscow, Atomizdat, 1974.

19. Nikolayev, V.B. ZHTF, 46, 1555 (1976).

20. Fenstermacher, C.A., Nutter, M.J., Leland, W.T. and Boyer, K. APPL. PHYS. LETTS., 20, 15 (1972).

21. Mills, C.B. J. APPL. PHYS., 45, 2112 (1974).

22. Douglas-Hamilton, D.H. and Mani, S.A. J. APPL. PHYS., 45, 4406 (1974).

23. Dipony, G., Perrier, F., Verdier, P. and Arnal, F. C.R. ACAD. SCI., PARIS, 258, 3655 (1964).

24. Yoder, M.J. and Ahous, D.R. APPL. PHYS. LETTS., 27, 673 (1975).

CSO: 1862
8831

LASERS AND MASERS

UDC 621.373.826.038.823

LASING MODES AND EMISSION CHARACTERISTICS OF A RING-TYPE PHOTODISSOCIATION IODINE LASER

Moscow KVANTOVAYA ELEKTRONIKA in Russian Vol 6 No 8, Aug 79 pp 1705-1711
manuscript received 27 Nov 78

[Article by V.N. Kurzenkov]

[Text] An experimental investigation is made of the energy, space-time and polarization characteristics of a photodissociation atomic iodine laser with a four-mirror ring cavity. It is shown that a key role in the formation of lasing directions is played by weak return signals which can arise in the absence of additional mirrors because of parasitic reflections or scattering. Under conditions of tube pumping a recording has been made of the influence of dynamic waves of inhomogeneities on the lasing threshold, which is evidenced in the space-time structure of the pattern of the close-range field. The linear nature has been established of polarization of the output emission in the absence of external magnetic fields. The feasibility is demonstrated of the employment for investigations of amplifying systems of a ring-type oscillator arrangement making possible suppression of the self-excitation of an amplifier employing cavity mirrors.

Theoretical and experimental investigations of the lasing modes of ring lasers (cf., e.g., [1-4]) have demonstrated that an important role in the lasing mechanism is played by the parameters and form of the amplification circuit, determined by the type of active medium, the amount of pumping and the level of return signals. In studies published up to the present time information is lacking on the properties of the ring circuit of an atomic iodine photodissociation laser (FL), which is of great interest because of the wide range of possible variation of its parameters. In this paper an experimental study is made of a number of characteristics of such a laser and measurements are made of energy conditions and properties of the output emission.

Experimental Setup

Measurements were made for the arrangement of a ring laser with a four-mirror cavity (fig 1). Serving as the active element was a quartz cell with Brewster windows with an inside diameter of 2.5 cm and an active section length of 25 cm,

placed in a two-lamp elliptical light source. The cell was filled with gaseous C_3F_7J or with mixtures of it with Xe at various pressures. The cavity was formed with three flat mirrors, M_2 to M_4 (R = 86 percent), and a glass plate, M_1, with a coated back surface. In one of the arms of the oscillator's outlet was installed an additional mirror, M_{dop}, whose reflection coefficient determined the lasing modes. Recordings were made of the energy (with calorimeters K_1 to K_4), time (with an FEU [photomultiplier]), polarization (with calorimeters K_2 and K_3), angular and spatial (with an EOP [image converter tube] and cameras F_1 and F_2) characteristics of the emission field. The emission spectrum was monitored individually; in the absence of a magnetic field lasing was performed along the single line $F = 3 \rightarrow F' = 4$ of the hyperfine structure of the $^2P_{1/2} - {}^2P_{3/2}$ transition.

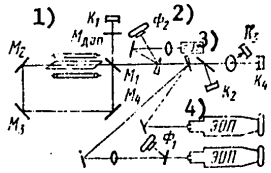

Figure 1. Sketch of Experimental Setup

Key:

1. M_{dop}
2. F_2
3. FEU
4. EOP

Experimental Results; Energy Characteristics

Measurements of the energy characteristics of a ring FL revealed the existence of stable single-wave and two-wave modes and an unstable mode with a change in lasing direction with a change in pressure of the working gas (fig 2).

Dependences, characteristic of the stable single-direction mode, of the output energy on the pressure of alkyl iodide are shown in fig 2a. The distribution of energy by direction in the absence of additional mirrors is of a fairly one-way nature (cf. W_1 and W_1'). The installation of an additional mirror with $R_{dop\ [additional]} = 4$ percent counter to the direction of W_1 changes the lasing direction to the opposite (cf. W_2 and W_2'). A reduction in R_{dop} results in a growth in W_2' and simultaneously in a decline in W_2. A distribution close to an equal-energy distribution (W_3 and W_3') was observed with $R_{dop} \approx 10^{-3}$. A smooth redistribution of intensity between directions in the direction of an increase in W_2' and a reduction in W_2 occurs also by gradual tilting of M_{dop}. It should be mentioned that in a number of cases the lasing direction without M_{dop} changed to the opposite after readjusting the arrangement, but in series with fixed adjustment the mode was stable and was reproduced well.

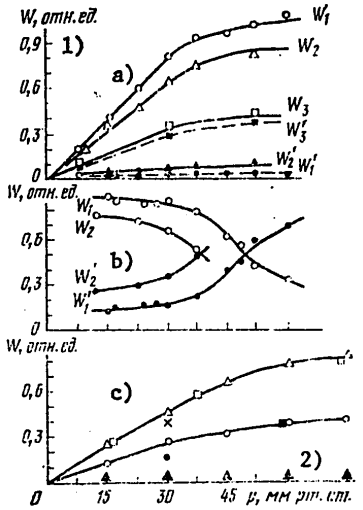

Figure 2. Dependences of Output Energy on Pressure of Alkyl Iodide in Stable Single-Direction Mode (a), in Mode with Unstable Lasing Direction (b) and in Stable Two-Wave Lasing Mode (c). In fig 2c are shown the following values:

W_1 (○), W_1' (▲), W_1^* (×), W_2 (□), W_3 (△), $W'3$(●); W_3^* (▣).

Key:
1. W , relative units
2. p , mm Hg

In the mode with an unstable lasing direction energy ratios had the form shown in fig 2b. The values of W_1 and W_1' represent the ratios of the output energy in the forward and reverse directions to the total energy. Instability is expressed in the redistribution of energy by direction (cf. W_1 and W_1') with a change in pressure of the alkyl iodide. When the arrangement was readjusted the nature of the distribution changed somewhat in form (cf. W_2 and W_2'). By adding a return mirror to arm W_1 with $p_{C_3F_7J}$ = 30 mm Hg equality of energies was achieved with $R_{dop} \approx 10^{-4}$.

Energy dependences relating to the stable two-wave mode are shown in fig 2c. In the presence of an additional mirror (R_{dop} = 4 percent , $R_{vykh\ [output]}$ = 10.7 percent) the generation is of a single-direction nature (cf. W_1 and W_1'), whereby energetically it is equivalent to the variant with a plane cavity (W_2 in fig 2c) with R_{vykh} = 8 percent . In the absence of M_{dop} ,

in each direction is contained about half the total energy (cf. W_3 and W_3'). Of definite interest is the fact that increasing the pressure of the active medium by the addition of a buffer gas (Xe, 150 mm Hg) for the purpose of achieving an amplification circuit of a purely homogeneous nature does not influence the lasing mode both without M_{dop} (W_3''), and with M_{dop} (W_1'').

Thus, the results of an experiment with an iodine FL have proven the possibility of the existence of all energy modes typical of a ring arrangement. It has been demonstrated that a substantial role in the formation of different modes is played by slight return reflections, and a change in modes is as a rule the consequence of a change in the system's parameters (a change of cells with readjustment of the cavity, or changes in the registration system).

Space-Time Characteristics of Emission

The shapes of lasing pulses were recorded integrally from the entire cross section of the active medium, and for the purpose of comparing typical modes they are given in fig 3. The high-amplitude pulse in fig 3a corresponds to an arrangement with R_{dop} = 4 percent , and the second pulse was recorded under the same conditions without M_{dop} in the stable two-wave mode. The parameters of pulses in the M_{dop} ring arrangement and in an arrangement with an ordinary two-mirror optical cavity practically did not differ. With the elimination of M_{dop} and a changeover to the two-wave mode, in addition to a reduction in the pulse's amplitude, there was evidenced slight modulation of its peak. A comparison of pulses propagated in opposite directions in the mode of practically single-direction generation without M_{dop} shows a drastic difference in their shapes (fig 3b). The lasing time is determined by the length of emission in the forward direction (the bottom pulse); in the reverse direction (the top pulse) in this interval were observed a single little peak or a series of several relatively short little peaks. The difference in the shapes of pulses demonstrates that the return signal is not a result of reflection of the forward, but is formed independently. In experiments with a return mirror were observed a slightly pronounced correlation, resulting from the great difference in amplitudes, in the origin of small peaks in the reverse direction and a slight reduction in amplitude in the forward direction, which possibly indicates the presence of the effects of competition.

A typical feature of the lasing pulse regardless of the type of cavity is its peak structure, partially observed on oscillograms and distinctly evidenced in the dynamics of the picture of the close-range field (fig 4). Measurements of the structure of the field in the close-range zone, made by means of a slit scan of the image on the EOP, demonstrated (fig 4a) that the modes studied are observed under conditions of fairly homogeneous pumping of the active medim (pressure of alkyl iodide less than or equal to 75 mm Hg). At the initial and final stages of the pulse are clearly pronounced pulsations in intensity with a period of approximately 1 μs. The period is variable over time and depends on the pumping level. Scanning of pulse sections with faster sweeps showed the presence of pulsations with a 100 percent modulation depth and a period of up to 10 ns (fig 4b), arising under conditions of a more than twofold excess in pumping over the threshold, synchronously with regard to cross section.

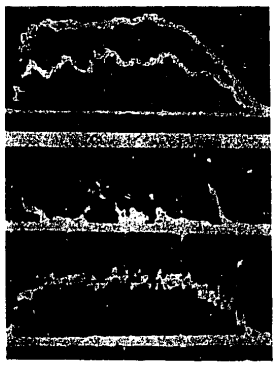

Figure 3. Oscillograms of Lasing Pulses: Sweep of 10 ms/division.

Figure 4. Slit Scan of Lasing Zone with a Scanning Duration of 50 μs (a) and Scan of Section of Lasing Zone (b)

Key:
1. 1 μs

In the scan of the emission field given in fig 4a is observed a zone of weakened intensity moving from the walls of the cell to its center at a rate of approximately 200 m/s. A similar pattern was clearly recorded in cases when the pressure of C_3F_7J or a mixture of it with Xe equaled approximately greater than 60 mm Hg. This fact can be explained by the presence of dynamic waves of inhomogeneity of an active medium in an FL with tube pumping [5,6]

and directly demonstrates their influence on lasing power, occasioned by a growth in the threshold in the shock zone.

It must be mentioned that the nature of the change in the width of the directivity diagram over time corresponded to the dynamics of the development of shock waves; this fact was evidenced in a growth in the width of the diagram over time with an increase in pressure of the active medium above 15 mm Hg. With lower pressures and the same pumping level the dispersion and emission remained practically constant for the period of the entire lasing pulse. This pattern was typical to an equal degree of both ordinary and ring cavities. In experiments with a ring cavity in individual instances was detected instability in the direction of the diagram's maximum over time, as a rule falling in line with the plane of the cavity, which is most probably related to conditions for the formation of lasing in an out-of-adjustment cavity with an inhomogeneous active medium. In the course of measurements of the width of the diagram while focusing the emission and comparing the dimensions of a spot at different distances from the focal plane was observed a distinctly pronounced hyperfocal focusing effect [7]. A spot of minimal dimensions with time-integrated radiation density practically an order of magnitude greater than the density in the focal plane was recorded (without optimization) at a distance of 30 to 50 mm beyond the focal plane of a lens with a focal length of 750 mm installed at a distance of 4 m from the outlet mirror. This fact testifies to the closeness to sphericity of the wave front in an FL with a cavity having plane mirrors in the presence of optical deformation of the active medium.

Polarization of Emission

An analysis of polarization of the output emission was made by comparing the energy of signals reflected from two mutually perpendicular Brewster's bands, M_3 and M_4 (cf. fig 1). The orientation of these bands corresponds to two separate directions: parallel to and perpendicular to the cavity's plane.

In an FL with an ordinary optical cavity the nature of polarization of the emission is determined wholly by the presence inside the cavity of a cell with Brewster windows. The polarization is in this case linear, its direction is determined by the orientation of the windows, and the measured ratio of components with regard to energy equals 10^2 and more. Another pattern is observed in an arrangement with a ring cavity. Regardless of the orientation of the Brewster windows, radiation was linearly polarized in relation to H in the cavity's plane. This fact demonstrates that the nature of polarization is determined by the ratio of amounts of feedback through the outlet mirror, which is confirmed by estimates of the corresponding threshold conditions. The reflection coefficients at an angle of 45° from the surface of a glass plate (the outlet mirror) for mutually orthogonal components equal R = 10.7 and 1.1 percent . A computation of threshold values of unsaturated gain for two orientations of the windows gives in the first instance 0.1 and 0.13 cm^{-1}, and in the second, 0.9 and 0.22 cm^{-1}. From comparison of these results one can understand the constancy in the direction of emission polarization in a ring FL with a glass plate as the outlet mirror. It should be mentioned that this feature of polarization can prove to be very important in a number of

instances. For example, in the presence of external magnetic fields there can be evidenced a dependence of lasing parameters on orientation of the field, and obviously in the most complex way in the case of a spectrally and polarizationwise inhomogeneous active medium.

Ring-Type Photodissociation Laser with an Amplifier

This arrangement makes possible optical bypassing with regard to reflections and makes it possible to eliminate self-excitation of an amplifier employing cavity mirrors, at the same time improving storable inversion in operation in the slave mode and making possible registration of the amplified signal in synchronous pumping. In experiments conducted these ideas were tested experimentally, whereby as the amplifier was used the active element of the FL described, and as the oscillator served a similar element with a cell of somewhat smaller diameter (1.5 cm). The typical pattern characterizing the operation of a system in the slave mode with an ordinary two-mirror cavity is shown in fig 5a. Two pulses were observed, the first of which relates to self-excitation of the amplifier with the oscillator's cavity mirrors and the second represents the amplified signal. The energy of the self-excitation pulse equaled, depending on the pumping level of the amplifier, from 20 to 50 percent of the stored energy. Self-excitation of the amplifier was practically totally eliminated when using in the system a ring cavity with an additional mirror fixing the lasing direction (R_{dop} = 4 percent). In this case in the emission is observed only an amplified pulse (fig 5b). Thus, it was possible either completely to eliminate the influence of the mirrors or to reduce it substantially, while maintaining the level of the input signal.

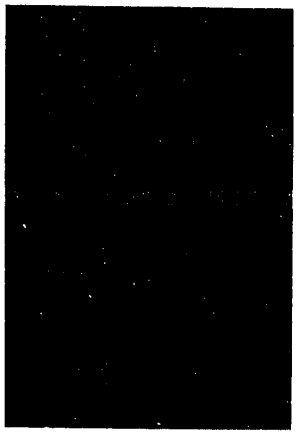

Figure 5. Oscillograms of Pumping Current of Amplifier and Oscillator (Top Beams) and of Emission Pulses in the Amplifier's Output (Bottom Beams). Sweep of 25 μs/division.

Discussion of Results and Conclusions

The results given demonstrate that in a ring-type iodine laser a practically single-direction lasing mode can be accomplished and can be steady without additional mirrors and barrier-layer devices. Of course, one of the possible reasons for its occurrence can be the effects of competition between counter waves, the simultaneous generation of which near the threshold at matching frequencies is impossible with expansion of the luminescence boundary of a uniform nature [2]. For an iodine FL with tube pumping these conditions can be assumed to be fulfilled [8,9], taking into account the fact that the pumping level is variable, i.e., a single-wave mode is possible at the moment of the origin of generation, when the pumping rate is not too high. It is known also from experiments with a ruby laser that single-direction generation is realized also with a sufficiently high excess in pumping over the threshold with the presence inside the ring cavity of an external control signal [10]. This provides a basis for assuming that a similar mechanism for the origin and evolution of single-direction generation is possible also in an iodine ring FL. However, the randomness in the generation direction characteristic of this variant has practically not been observed.

As demonstrated by experiments with an additional mirror, quite important to the formation of energy distributions is the influence of weak return signals, whose role for conditions closest to the experimental was analyzed in [4]. It was demonstrated in [4] that with the presence of slight feedback in one direction a counter wave evolves, if its initial amplitude is sufficiently great; otherwise a single-wave mode is stable. In the experiment for this, obviously sufficient is the presence of parasitic reflections or scattering, which additionally supply the counter wave, in confirmation of which can be given the experimental result of [3], where reflection from the faces of the active element, having arisen when their tilt was eliminated, resulted in a two-wave generation mode. With the presence of an additional mirror generation according to [4] must be of a single-wave steady-state nature with a direction determined by this mirror, in the case when $R_{dop} > R_{kr}$, where R_{kr} is the critical value depending on the pumping level. Under the conditions of the experiment the excess in pumping over the threshold equaled 2 to 2.5 and with $R_1 = 0.107$ and $R_{2-4} = 0.86$ the calculatinon gives $R_{kr} = 3$ to 4 percent, which is in total agreement with the experiment: With $R_{dop} =$ = 4 percent was observed a stable practically single-direction generation mode. Taking these facts into account, the hypothesis regarding the features of the formation of energy modes realized in experiments with a ring-type iodine FL can be formulated in the following manner.

1) The reason for the origin of a specific mode is difficult-to-monitor redistributions, characteristic of a specific arrangement, in the magnitude and ratios of weak return signals, which in the absence of additional mirrors can be formed as the result of parasitic reflections or scattering, e.g., in windows of a cell contaminated by photolysis products,

2) The existence of a stable single-direction mode is apparently associated with the presence of return signals which are weak (approximately 10^{-3}) but different in magnitude,

3) The presence of an unstable mode with a change in generation direction with a change in pressure of the active medium is possibly caused by return signals which are weaker as compared with the preceding case and close in magnitude, and by the simultaneous effect of variable amplification parameters.

4) The stability of the two-wave mode, as in [3], can evidently be explained by the presence of parasitic reflections which are considerable and comparatively close in magnitude. Thus, the results presented demonstrate that the kinetics of the generation of a ring-type iodine FL depend substantially on the presence in the system of parasitic signals whose influence has been recorded experimentally at a level of approximately 10^{-4}; therefore, for the purpose of isolating in pure form controllable effects in the competition of counter waves it is necessary to take special measures for the suppression of these signals. Of definite practical interest is single-direction generation without additional mirrors, as well as with an additional mirror with $R_{dop} << 1$, which can be used as a variant of optical bypassing with regard to reflections in amplification systems for the purpose of eliminating self-excitation. The suppression of generation in the dynamic shock wave zone detected in measurements of space-time characteristics of the emission demonstrates the direct influence of these waves on the generation threshold of an FL under conditions of pumping with pulsed tubes, which must be taken into account in a detailed discussion of generation kinetics in addition to features of polarization specific to a ring-type FL system and evidenced in the most complex manner in the presence of external magnetic fields.

In conclusion, the author expresses his gratitude to N.N. Rozanov for his helpful discussion of several questions in this paper, and also to I.M. Belousova for a number of practical valuable recommendations.

Bibliography

1. Tang, G.L., Statz, H., de Mars, C.A. and Wilson, D.T. PHYS. REV., 136, 1 (1964).

2. Zeyger, S.G. and Fradkin, E.Ye. OPTIKA I SPEKTROSKOPIYA, 21, 386 (1966).

3. Bonch-Burevich, A.M., Petrun'kin, V.Yu., Yesepkina, N.A., Kruzhalov, S.V., Pakhomov, L.N., Chernov, V.A. and Galkin, S.L. ZHTF, 37, 2031 (1967).

4. Rozanov, N.N. OPTIKA I SPEKTROSKOPIYA, 38, 340 (1975).

5. Golubev, L.Ye., Zuyev, V.S., Katulin, V.A., Nosach, V.Yu. and Nosach, O.Yu. KVANTOVAYA ELEKTRONIKA, edited by N.G. Basov, No 6 (18), 23 (1973).

6. Danilov, O.B., Novoselov, V.V. and Spiridonov, V.V. OPTIKA I SPEKTROSKOPIYA, 39, 680 (1975).

7. Malayev, V.V. and Kaliteyevskiy, N.I. In "Fizika gazovykh lazerov" [Physics of Gas Lasers], Leningrad, Izdatel'stvo LGU, 1969, p 5.

8. Zuyeyev, V.S., Katulin, V.A., Nosach, V.Yu. and Nosach, O.Yu. ZHETF, 62, 1673 (1972).

9. Belousova, I.M., Kiselev, V.M. and Kurzenkov, V.N. OPTIKA I SPEKTROSKOPIYA, 33, 210 (1972).

10. Antsiferov, V.V., Derzhi, N.M., Kuch'yanov, A.S., Pivtsov, V.S., Ugozhayev, V.D. and Folin, K.G. KVANTOVAYA ELEKTRONIKA, 2, 57 (1975).

CSO: 1862
8831

LASERS AND MASERS

UDC 612.378.325

INVESTIGATION OF PROPERTIES OF A LASER WITH AN UNSTABLE CAVITY AND ADDED FEEDBACK

Moscow KVANTOVAYA ELEKTRONIKA in Russian Vol 6 No 8, Aug 79 pp 1773-1775
manuscript received 9 Jan 79

[Article by Yu.A. Anan'yev, D.A. Goryachkin, N.A. Sventsitskaya and I.M. Petrova]

[Text] An experimental study is made of the properties of a laser with an unstable cavity and an added mirror covering part of the cross section of the light beam for the purpose of lowering the lasing threshold. The results are compared with the case of an ordinary unstable cavity of low magnification. It is shown that in a laser with an unstable cavity and added feedback it is impossible to achieve low angular divergence of the radiation.

If to a laser with an unstable cavity is added an additional element (mirror or semitransparent plate), as the result of reflection from which a converging wave is formed, this results in an increase in the radiation density in the zone near the axis and in lowering of the lasing threshold [1,2]. Both can prove to be useful in different practical applications.

Increasing the density in the zone near the axis facilitates control of the laser by means of influencing the small central area of its cross section, which can be used in particular for accomplishing the spectral selection of radiation [2]. The effect of lowering the lasing threshold in principle makes it possible to use unstable cavities, least critical with regard to accuracy of fabrication, adjustment and the like, with high magnification, M , not only in ordinary cases, but also for lasers with not too great amplification in the active medium. At the same time in all previous experiments [1,2] the addition of a supplementary element caused, in addition to desirable consequences, also an increase, completely unacceptable from the viewpoint of practical application, in the angular divergence of the radiation. In [2] this was explained by the existence of an entire series of ray trajectories which became "locked" because the added reflector covered the entire cross section of the cavity. This paper is devoted to a study of the interesting case when the added reflector covers only such a portion of the cross section that the existence of locked trajectories within the framework of a geometrical approximation becomes impossible.

Experiments were performed with a neodymium glass laser (diameter of active element 45 mm, length 600 mm), operating in the free generation mode. In order to imitate the case of media with low amplification, only a part of the active element 200 mm long was subjected to pumping. Under these conditions the optical magnification, M , of an ordinary telescopic cavity (without an added reflector) equaled 1.2 to 1.3; the use of such a cavity with $M = 1.26$ made possible an output energy of approximately 30 J and angular divergence of the radiation (in terms of the half-energy level) of approximately 1.5'. With an ordinary cavity with $M = 2$ the lasing threshold is barely reached.

In experiments with a flat supplementary reflector installed at the outlet of the telescopic cavity, both the reflection coefficient of the reflector, ρ ($\sim$ 100 and $\sim$ 10 percent), and the magnification of the cavity ($M = 2$, 3.8 and 8.3) were varied. By moving the reflector transversely it was possible to change the area of the covered portion of the cavity's cross section (the boundary of the reflector located within the working cross section was a straight line). The majority of measurements were performed with a reflector covering half or not much less than half of the cross section; the "geometrical" modes described in [2] hereby certainly were not able to be formed.

It was shown that the addition of a supplementary reflector lowers the lasing threshold quite heavily. Not only with $M = 2$ ($\rho \sim 100$ and ~ 10 percent) but even with $M = 3.8$ ($\rho \sim 10$ percent) the output energy was even somewhat greater than 30 J, and only in the case of $M = 8.3$ and $\rho \sim 100$ percent did it drop to 12 J. Moreover, the amount of angular divergence did not once drop below 2', sometimes reaching 4.5' ($M = 2$, $\rho \sim 100$ percent). From this follows the main conclusion that it is obviously impossible to achieve satisfactory results in unstable cavities with a forcibly formed converging wave. Even very simple unstable cavities with not too high M prove to be more advantageous from the viewpoint of angular divergence of the radiation; it is not necessary even to speak of investigations in [3,4] of unstable cavities with rotation of the field.

Let us relate some more useful information on the behavior of lasers with a supplementary reflector. In fig 1 is shown a picture of the angular distribution of radiation in the case when $M = 2$ and $\rho \sim 100$ percent (the reflector covers slightly less than one half the cross section). If this picture is compared with the similar one for the case of a cross section totally covered by a semi-transparent reflector [2], then it can be seen that the first of these represents, as it were, one half of the second--in the angular distribution are seen the same rings with the diameter of each succeeding one M-fold greater than the diameter of the preceding one.

Similar patterns of angular distribution were observed also in a passive experiment, a sketch of which is shown in fig 2. A parallel beam of light from an auxiliary gas laser ($\lambda = 0.63$ μ) was directed through dividing plate 3 onto concave mirror 1 of the telescope formed by totally reflecting mirrors 1 and 2. At the outlet of the telescope in the remote zone (through telescope 4) is seen a system of rings whose diameters, as before, increase successively

M-fold. If one half the cross section of the original beam is covered, then the aperture around the convex mirror in the telescope's outlet is all the same illuminated completely, whereas in the remote zone only half of the original pattern remains.

Figure 1. Angular Distribution of Radiation of a Laser with an Unstable Cavity (M = 2) and a Supplementary Mirror in Part of the Cross Section

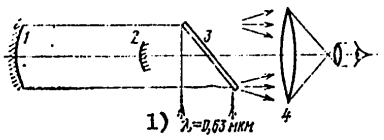

Figure 2. Sketch of Passive Experiment

Key:
1. $\lambda = 0.63\ \mu$

All this testifies to the fact that the attempt made in [2] to explain phenomena arising in adding a supplementary reflector on the basis of notions of purely geometrical optics was illegitimate. When the converging wave produced by the reflector (or external source) completes several passes through the telescope system and its cross section is reduced many times, diffraction takes on a decisive role. Diffraction "spreading" of the beam (conducive to which can be the influence of inhomogeneities in the medium) results in the fact that part of the radiation goes back and part penetrates from one half of the cross section into another. These processes are completely similar to the processes, considered in [5,6], of reflection from a caustic and of the passage through it of converging waves produced by diffraction at the edge of the cavity. As a result in precisely the same way is evidenced the degeneration of modes with respect to losses, a tendency toward multimode generation, and, as a result, a growth in divergence of the radiation. Of course, with the addition of a reflector, on account of the high intensity of converging waves, all these undesirable consequences turn out to be

immeasurably greater than in the case when the only source of converging waves is edge diffraction.

From the results of passive experiments can be concluded also the lack of promise of attempts to control the radiation of a laser with an unstable cavity by introducing converging waves from an external source (a suggestion of this kind was made, in particular, in [7]). Requiring a quite cautious attitude is also the question of using multi-pass telescopic amplifiers in experiments with return of the wave front; in the performance of passive experiments according to the diagram in fig 2 the system of rings in the remote zone is visible even in the case when in the concave mirror there is an opening whose diameter is greater than the diameter of the convex mirror.

Bibliography

1. Anan'yev, Yu.A., Vinokurov, G.N., Koval'chuk, L.V., Sventsitskaya, N.A. and Sherstobitov, V.Ye. ZHETF, 58, 786 (1970).

2. Anan'yev, Yu.A., Grishmanova, N.I., Petrova, I.M. and Sventsitskaya, N.A. KVANTOVAYA ELEKTRONIKA, 2, 738 (1975); 2, 1952 (1975).

3. Zavgorodneva, S.I., Kuprenyuk, V.I. and Sherstobitov, V.Ye. KVANTOVAYA ELEKTRONIKA, 4, 1383 (1977).

4. Anan'yev, Yu.A. PIS'MA V ZHTF, 4, 372 (1978).

5. Vinokurov, G.N., Lyubimov, V.V. and Orlova, I.B. OPTIKA I SPEKTROSKOPIYA, 34, 741 (1973).

6. Anan'yev, Yu.A. and Sherstobitov, V.Ye. ZHTF, 43, 1013 (1973).

7. Buczek, C.J., Frieberg, R.J. and Scolnik, M.L. PROC. IEEE, 61, 1411 (1973).

CSO: 1862
8831

LASERS AND MASERS

UDC 621.373.826

SOME RESULTS OF EXPERIMENTS ON A GAS DYNAMICAL CO_2 LASER

Moscow KVANTOVAYA ELEKTRONIKA in Russian Vol 6 No 8, Aug 79 pp 1775-1777
manuscript received 21 Jan 79

[Article by S.B. Goryachev, B.A. Tikhonov and V.F. Sharkov, Institute of Atomic Energy imeni I.V. Kurchatov, Moscow]

[Text] The results are given of preliminary experiments on a CO_2 GDL [gas dynamical laser] with heating of the working mixture of gases N_2-CO_2-He in a plasmatron. In the continuous operation mode arrived at experimentally are a unit power output of 20 J/g and an efficiency of approximately 1.2 percent with a stagnation temperature of $T_0 = 1700 \pm 100°K$, a value of parameter p_0h^* of approximately less than 0.5 atm·cm and a total gas mixture flow rate of approximately 0.5 kg/s.

Up to the present time in numerous experiments with homogeneous CO_2 GDL's [1] not too high levels have been obtained, as compared with those predicted by the theory, in such key laser characteristics as efficiency and unit power output. In the stagnation temperature range of practical importance, $T_0 = 1700 \pm 100°K$, instead of the calculated efficiency of greater than one percent and unit power output of 20 to 30 J/g, obtained experimentally have been an efficiency of approximately 0.1 to 0.5 percent and a unit power output of approximately less than 10 J/g.

In this paper are reported some results of experiments with the unit in [2], the modernized arrangement of which is shown in fig 1. This is a stationary wind tunnel with the separate delivery from high-pressure cylinders of technically pure nitrogen, helium and carbon dioxide. Part of the nitrogen passes through a three-phase plasmatron [3,4], where it is heated to approximately 400°K. The prescribed stagnation temperature with a certain percentage composition of the working gas mixture is obtained by mixing in the gas channel behind the plasmatron the required quantities of cold nitrogen, helium and carbon dioxide. Furthermore, since the area of the nozzle's critical cross section is fixed, is set a specific stagnation pressure, p_0 ·3 The spent gas mixture is exhausted into a vacuum tank with a volume of 50 m^3, which has been preliminarily evacuated to 0.1 to 1 mm Hg.

The throat unit is assembled from 52 flat profiled fins similar to those described in [1,2], which form 51 supersonic throats with a critical cross section of 0.047 X 5.1 cm and an expansion ratio of 22 each. The dimensions of the supersonic vacuum channel are 50 X 50 cm with a height which varies along the stream from 5.1 to 7 cm for the purpose of compensating the growth of the boundary layer. A cavity of the stable type is formed by an opaque concave copper mirror (diameter of 15 cm and radius of curvature of optical surface of 15 m) and by a plane-parallel semi-transparent germanium mirror (diameter 15 cm and thickness of 2.2 cm). The distance for the flow from the critical cross section to the axis of the cavity is 25 cm. The semi-transparent mirror on one surface has a dielectric translucent coating, and on the other, facing the opaque mirror, a dielectric reflecting coating with a reflection coefficient of 80 $\pm$ 3 percent. For the purpose of relieving the semi-transparent mirror of atmospheric pressure, the beam is led out through a plate of KCl 2 cm thick. The cross section of the extracted beam at a distance of 20 cm from the outlet plate has dimensions of 14 X 5 cm. The length of the working pulse is 1.2 s $\pm$ 2 percent. The time for the buildup and release of pressure is 0.1 s for each. The laser energy derived during the time of a working pulse was measured by a calorimeter with a thermistor. The duration and shape of the lasing pulse were monitored with an FSG-22-3A2 photoconductive cell.

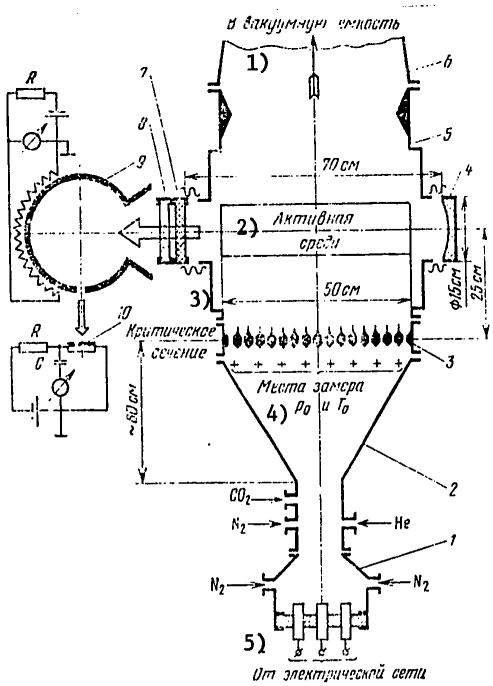

Figure 1. Sketch of Experimental Unit: 1--plasmatron; 2--mixer-reducer; 3--throat unit; 4--adjusting unit with opaque copper mirror;
[Caption continuation and key on following page]

5--supersonic vacuum channel with exit cone; 6--exhaust manifold; 7--adjusting unit with semi-transparent germanium mirror; 8--KCl vent plate; 9--calorimeter with thermistor; 10--photoconductive cell

Key:
1. To vacuum tank
2. Active medium
3. Critical cross section
4. Points for measuring p_0 and T_0
5. From electrical main

As a result, with $T_0 = 1700 \pm 100°K$, $p_0 = 6.5$ to 8.5 atm, a working gas mixture flow rate of 550 to 750 g/s, and a molar composition of the gas mixture of N_2:He:CO_2 = 45:45:10, the unit power output averaged per second equaled 20 ± 3 J/g, and the efficiency approximately 1.2 percent. The total number of experiments for which statistical processing of the results was carried out equaled approximately 300.

While varying the reflection coefficient of the outlet mirror (the remaining parameters of the unit remained the same), an experimental measurement was made of the value of the unsaturated gain: $K_0 = 1 \pm 0.3\ m^{-1}$.

Two series of experiments were also performed in which, while maintaining the specified composition of the working gas mixture and identical operating parameters of the unit, in the plasmatron was heated either a molecular gas--nitrogen--or a monoatomic gas--helium--and the remaining components of the mixture were mixed in the mixer-reducer. The measured values of the unit power output in both series of experiments proved, with an accuracy of not worse than 20 percent, to be identical, which indicates the equilibrium nature of heating of the gas in the plasmatron (for our conditions) and, consequently, the possibility of extending the data obtained to a CO_2 GDL with an arbitrary method of heating the working mixture.

Thus, in our experiments energy characteristics were obtained for a CO_2 GDL which exceed the values obtained under comparable conditions in [1]. The key physical reasons responsible for obtaining rather high values of unit power output are apparently the following:

1) The organization of the gas stream both in the supersonic section of the throat unit and in its subsonic part, especially the elimination of overflows of small quantities of the heated gas working mixture past critical cross sections of throats.

2) Elimination of the influence of heating of throat fins and cavity mirrors by employing relatively short-duration working startups for the unit (approximately 1 s).

3) The employment as components of the working mixture of technically pure gases, N_2, CO_2 and He.

4) Ensuring in all experiments values of parameter p_0h of not greater than 0.5 atm·cm.

5) Placement of the optical cavity at an optimal distance from the throat unit (approximately 20 cm), i.e., beyond the zone of companion traces [1] of the throat fins.

6) High quality of the cavity's mirrors (the opaque mirror, e.g., had a reflection coefficient of not less than 98.5 percent).

In addition, as preliminary numerical studies demonstrated, the composition of the working gas mixture, CO_2:N_2:He = 10:45:45, and the reflection coefficient of the outlet mirror, R = 80 percent, are quite close to the optimal parameters enabling maximum unit power output.

It is necessary, however, to emphasize that only after comprehensive experimental and theoretical optimization of the unit's parameters, which it has been proposed to carry out in the future, possibly, will it be possible to refine the energy balance in the GDL and determine unambiguously the quantitative influence of the numerous operating parameters on the specific power output of a CO_2 GDL.

The authors wish to mention the constant attention to this paper of Ye.P. Velikhov and V.D. Pis'mennyy, the participation of M.Yu. Orlov, F.G. Rutberg, M.A. Grigor'yev and Yu.F. Suslov in the creation of experimental equipment, as well as the valuable comments of G.V. Abrosimov, A.A. Belokon', A.M. Dykhne, A.N. Kukhto, A.P. Napartovich and E.L. Spektor, made in discussions of experimental results and wish to express their thanks to them.

Bibiliography

1. Losev, S.A. "Gazodinamicheskiye lazery" [Gas Dynamical Lasers], Moscow, Nauka, 1977.

2. Abrosimov, G.V., Vedenov, A.A., Vitshas, A.F., Napartovich, A.P. and Sharkov, V.F. TVT, 13, 865 (1975).

3. Glebov, I.A., Kasharskiy, E.G. and Rutberg, F.G. "Sinkhronnyye generatory v elektrofizicheskikh ustanovkakh" [Synchronous Generators in Electrophysical Units], Leningrad, Nauka, 1977.

4. Brantsev, A.N., Grigor'yev, M.A., Kiselev, A.A. and Rutberg, F.G. "Moshchnyye generatory nizkotemperaturnoy plazmy i metody issledovaniya ikh parametrov" [High-Power Low-Temperature Plasma Generators and Methods of Investigating Their Parameters], Leningrad, Trudy VNIIElektromash, 1977.

CSO: 1862
8831

LASERS AND MASERS

UDC 621.375.826;539.196.5

EFFICIENCY OF A SELECTIVE CO LASER

Moscow KVANTOVAYA ELEKTRONIKA in Russian Vol 6 No 8, Aug 79 pp 1816-1818
manuscript received 17 Jan 79

[Article by A.A. Likal'ter, USSR Academy of Sciences Institute of High Temperatures, Moscow]

[Text] For a CO laser with a selective cavity are found the generating transition efficiency and the gain saturation law. The efficiency of selective lasing is limited by the transfer by molecules of quanta to the upper portion of the vibrational spectrum in eluding the lasing transition.

A CO laser generates simultaneously in several vibrational-rotational bands from 5 to 8 μ. In order to isolate radiation at a single frequency, a selective cavity is employed. The efficiency of a CO laser with a selective cavity was studied experimentally in [1] and a theoretical estimate is given in [2]. In this paper the specifics of selective generation are taken into account more completely. A limiting factor for efficiency is shown to be the transfer by molecules of quanta into the upper portion of the vibrational spectrum in eluding the lasing transition.

A study has been made of the flow of excitation quanta in the vibrational spectrum, corresponding to localization of pumping in the lower half and of quenching in the upper half of the spectrum [3,4]. The flow of quanta is carried by the vibrational-vibrational (VV) transfer $CO(\ell) + CO(u + 1) \rightarrow CO(\ell + 1) + CO(u)$, enabling the transfer of excitation from transition $(u) - (u + 1)$ to the transition $(\ell) - (\ell + 1)$. The flow of quanta in the section passing through level v is determined by the equation

$$\Pi_v = \sum_{u<v} \sum_{l \geqslant v} Q^{u+1,u}_{l,l+1} \left(n_l n_{u+1} - e^{-2b(l-u)} n_{l+1} n_u\right), \tag{1}$$

where n_ℓ is the population density of vibrational level ℓ; $b = x\omega/T$, where $x\omega$ is the anharmonicity constant and T is the temperature.

The rate constant for VV exchange is represented in the form

$$Q^{u+1,u}_{l,l+1} = Q(u+1)(l+1)e^{-\delta(l-u)} \quad (l>u),$$

where Q and δ are parameters. If the characteristic length of the variation in population density on the vibrational number axis is much greater than the mean free path of a quantum, then the flow of quanta is expressed in differential form:

$$\Pi = (2Q/\delta^3)v^2n^2[2b - d^2\ln n/dv^2]. \tag{2}$$

The distribution satisfying the boundary conditions and consistent with constant P has the form [5]:

$$n = \begin{cases} n_0 \exp(-2b\alpha v + bv^2), & v < \alpha; \\ (n_0\alpha/v)\exp(-b\alpha^2 - 1/2), & \alpha < v < N, \end{cases} \tag{3}$$

where α is the coordinate of Treanor's minimum and N is the boundary of the region in which VV exchange dominates.

The corresponding value of the quanta flow is

$$\Pi = (4bQ/\delta^3)v^2n^2, \tag{4}$$

where n is determined by equation (3) with $v > \alpha$. Under steady-state conditions the flow of quanta is equal to the difference in pumping and losses in the Treanor section of the distribution with $v < \alpha$. We will not dwell on taking into account the different losses at the plateau when $v > \alpha$.

Beyond the lasing transition at point γ (fig 1) the flow of quanta is reduced to a finite value equal to the number of de-excited laser quanta. It is necessary to relate the discontinuity in the flow to the derivative $d \ln n/dv$ at point γ; this is expressed through the gain.[2] The discontinuity in the flow causes a discontinuity in derivative $d^2 \ln n/dv^2$. In connection with this, diffusion representation (2), generally speaking, is not valid in the vicinity of point γ with a radius less than the length of the quantum's mean free path. In extending equation (2) to this vicinity, it is necessary to add a certain effective boundary condition. Its role is played by an additional relationship obtained from (1). Abbreviating in difference $P_v - P_{v+1}$ terms making a contribution to the flow in both cross sections, and going to a differential representation, we find

$$\Delta\Pi = (\delta/2)\Delta\Pi_D, \tag{5}$$

where ΔP and ΔP_D are the real and diffusion discontinuities in the flow, respectively, in the lasing transition; factor $\delta/2 \sim 1/3$, equal to the inverse mean free path of a quantum, takes into account the transfer of quanta to the lasing transition bypass.

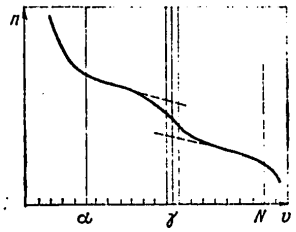

Figure 1. Vibrational Distribution in Vicinity of Lasing Transition

In computing the diffusion discontinuity in the flow we assume that the reduction in the level of the plateau associated with it is not too great. Regarding $y = \ln n$ as a coordinate, and vibrational number v as time, we write (2) in the form of an equation of motion of a particle above a potential barrier, depending on P as on a parameter:

$$\ddot{y} = -dU/dy,$$
$$U(v,y) = -2by - (\Pi\delta^3/4Qv^2)e^{-2y}.$$

The distribution satisfying the conditions of a non-negative character in this region and of diminution with high v corresponds to the trajectory of a particle almost entrapped by the peak of the barrier. (Since equilibrium at the peak of the barrier is unstable, other trajectories deviate heavily from the latter beginning with a certain v; therefore they cannot satisfy the necessary conditions.) Near the peak of the barrier the equation of motion has the form

$$\ddot{y} = 4b(y - y_p), \tag{6}$$

where

$$y_p = \frac{1}{2}\ln\frac{\Pi\delta^3}{4bQv^2}.$$

The general solution to equation (6)

$$y = y_p + Ae^{-2\sqrt{b}v} + Be^{2\sqrt{b}v} + \sum_{l\geq 1}\frac{(2l-1)!}{(2\sqrt{bv})^{2l}} \tag{7}$$

describes the vibrational distribution near the level of the plateau to which corresponds $y = y_r$.

Considering lasing at a transition localized with a fairly high vibrational number, we will assume that $2\sqrt{b}\gamma >> 1$ and we will let the asymptotic series descend in relation to the inverse powers of this parameter in (7). Coefficients A and B are found from the boundary conditions for each of the regions $\alpha < v < \gamma$ and $\gamma < v < N$, whereby with $2\sqrt{b}(\gamma - \alpha) >> 1$ and $2\sqrt{b}(N - \gamma) >> >> 1$ fulfillment of the boundary condition at the left end of each region is made possible by a term with a descending power, and at the right, with an ascending. In the vicinity of point γ the distribution has the form

$$n = \begin{cases} \sqrt{\frac{\Pi\delta^3}{4bQv^2}} \exp\left[\frac{\dot{y} + 1/\gamma}{2\sqrt{b}} e^{2\sqrt{b}(v-\gamma)}\right], & v < \gamma; \\ \sqrt{\frac{\Pi'\delta^3}{4bQv^2}} \exp\left[-\frac{\dot{y} + 1/\gamma}{2\sqrt{b}} e^{-2\sqrt{b}(v-\gamma)}\right], & v > \gamma, \end{cases} \tag{8}$$

where $\dot{y} = \dot{y}(\gamma)$ and P and P' are the flows of quanta with $v < \gamma$ and $v > \gamma$, respectively. Joining equations (8) with $v = \gamma$, we find the relationship of diffusion flows:

$$\Pi' = \Pi \exp\left[2(\dot{y} + 1/\gamma)/\sqrt{b}\right]. \tag{9}$$

From (9) and (5) follows the expression for the efficiency of the transition:

$$\eta = (\delta/2)\{1 - \exp\left[2(\dot{y} + 1/\gamma)/\sqrt{b}\right]\}. \tag{10}$$

The limiting value of the efficiency, $\delta/2$, is caused by the transfer of quanta into the lasing transition bypass. With a relatively not too great diffusion discontinuity in the flow

$$\eta = -\delta(\dot{y} + 1/\gamma)/\sqrt{b}, \tag{11}$$

Derivative $\dot{y}$ is expressed via the gain

$$K = \sigma_\gamma(j) n_\gamma (2Bj/T + \dot{y}), \tag{12}$$

where $\sigma_\gamma(j)$ is the cross section of the radiation gain in terms of the population density of the vibrational level; B is the rotational constant; and j is the rotational moment. Here it is assumed that $Bj/T << 1$. With not too high transition efficiency

$$\frac{K}{K_0} \approx \frac{2Bj/T + \dot{y}}{2Bj/T + 1/\gamma}, \tag{13}$$

where K_0 and K are the gain of a weak signal and the threshold gain, respectively. Expressing $\dot{y}$ from (13) and substituting it in (11), we find the relationship between the transition efficiency and measured values of K_0 and K:

$$\eta = \frac{\delta}{\sqrt{b}} \cdot \left(\frac{2Bj}{T} - \frac{1}{\gamma}\right)\left(1 - \frac{K}{K_0}\right). \tag{14}$$

The relationship between the gain and the intensity of radiation in the cavity is determined by the energy balance:

$$\eta \Pi \omega_\gamma = KI,$$

where I is the intensity of radiation and ω_γ is the laser quantum. Utilizing (14) we get the typical saturation law

$$K = K_0/(1 + I/I_s),$$

where

$$K_0 = \frac{\sigma\gamma}{\gamma}\sqrt{\frac{\Pi\delta^3}{4bQ}}\left(\frac{2Bj}{T} - \frac{1}{\gamma}\right); \quad I_s = \frac{2\omega\gamma\gamma}{\sigma\gamma}\sqrt{\frac{Q\Pi}{\delta}}.$$

In a non-selective cavity the change in the flow of quanta in the region of lasing transitions can be considered continuous and the efficiency of a single band can be defined as $\eta_\gamma = -(d \ln P/dv)_{v=\gamma}$. Utilizing equation (4) we have

$$\eta_\gamma = -2(\dot{y} + 1/\gamma). \tag{15}$$

This equation must be averaged on a length on the order of the mean free path of a quantum. In [2] an approximation similar to (15) (in a difference representation) is used also in selective lasing. Equation (11) for transition efficiency in selective lasing differs from (15) by the factor $\delta/(2\sqrt{b})$, depending on temperature.

In a sequence of lasing transitions a flow of quanta can be de-excited practically totally, which explains the high efficiency of a CO laser. On the other hand, lasing efficiency in a selective laser cavity is limited. Estimates according to equation (14) make it possible to explain the reduction observed

in [1] in the efficiency of a selective CO laser as compared with an ordinary one. The growth noted there in the radiated power of bands in the upper portion of the lasing spectrum in a selective cavity is related to an increase in the inflowing flow of quanta in the absence of lasing at lower-lying transitions, as well as to an increase in the transition efficiency.

The electro-optical efficiency of a laser is represented by the product of factors taking into account losses of energy at various stages. In addition to the losses taken into account by equation (14) they include the following: the excitation of electronic degrees of freedom; radiation, diffusion toward walls and VT exchange of molecules at vibrational levels below the lasing transition; dissipation in VV exchange, described by the quantum efficiency, ω_γ/ω, where ω_γ is the vibrational quantum of CO (or of N_2 if pumping takes place through nitrogen); and radiative losses in the cavity. Taking these losses into account for a selective CO laser is non-specific, i.e., is of a fairly general nature and therefore is not considered here.

Bibliography

1. Avtonomov, V.P. et al. KVANTOVAYA ELEKTRONIKA, 5, 1896 (1978).

2. Napartovich, A.P., Novobrantsev, I.V. and Starostin, A.N. KVANTOVAYA ELEKTRONIKA, 4, No 10 (1977).

3. Likal'ter, A.A. PMTF, No 4, 3 (1976).

4. Zheleznyak, M.B., Likal'ter, A.A. and Naydis, G.V. PMTF, No 5, 11 (1976).

5. Brau, C.A. PHYSICA, 58, 533 (1972).

CSO: 1862
8831

END